Examples of analyzing MPGD data

with emphasis on precise timing

PART II

- Extrapolate to the Invisible
- Use timing to examine charge properties and use charge to combine timing measurements
- The last Example: Response to a single photoelectron

Extrapolate to the Invisible

An Advertisement as an introduction

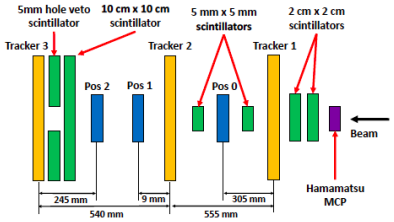

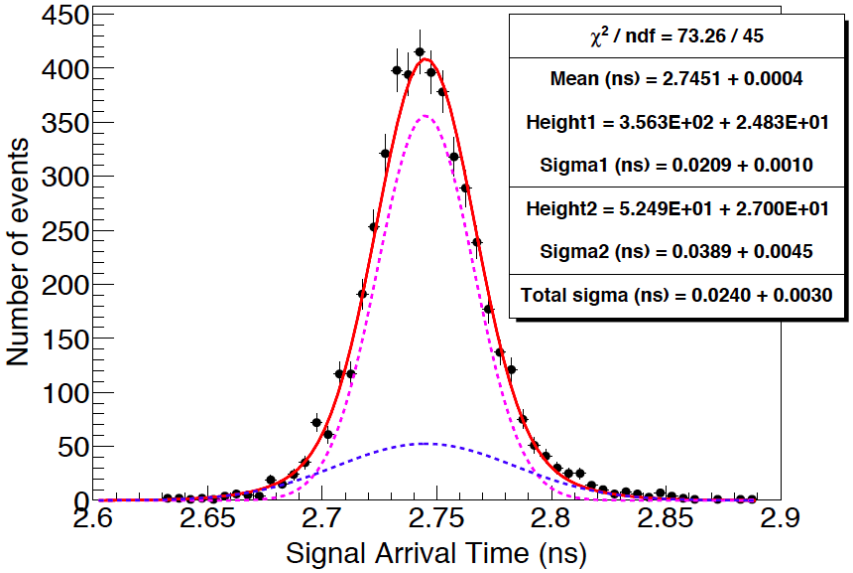

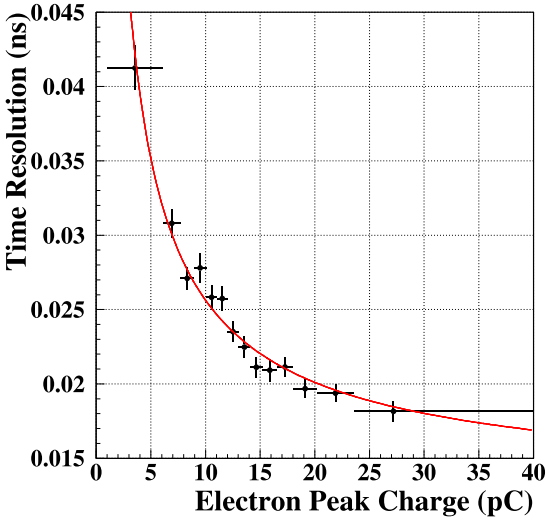

- **Why the Δt distribution is not Gaussian ?**
- **How we combine two Gaussians to calculate the total sigma ?**
- **What about if there were ten Gaussians with different mean and sigma values?**

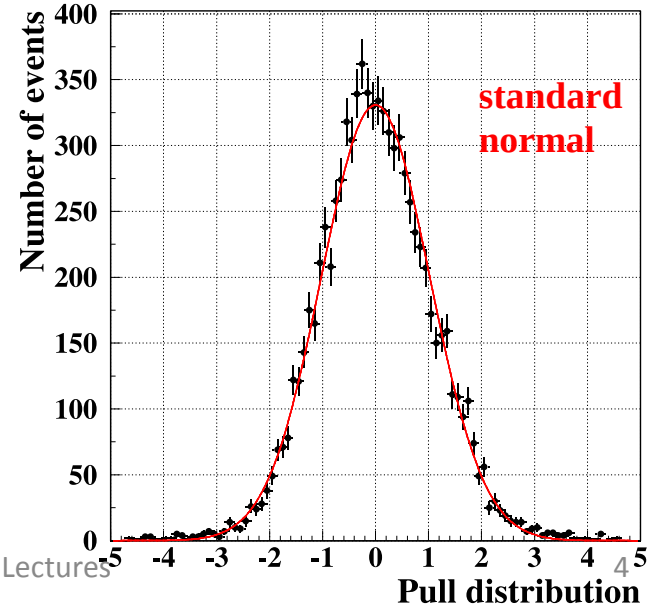

Another Timing Example (Extrapolating to the Invisible)

We have measured the PICOSEC response to a single pe using laser beam.
The timing resolution, estimated from these data, corresponds to a part only (the "visible" part) of the charge spectrum.

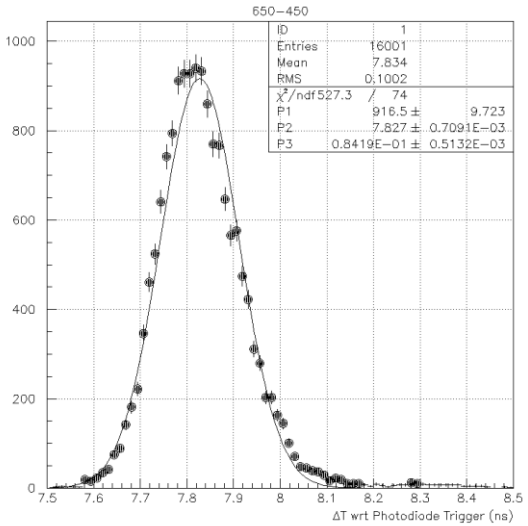

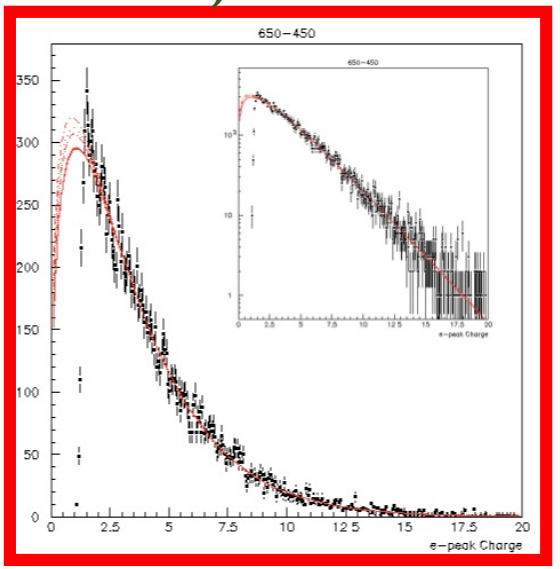

We have measured the mean signal arrival time and the related timing resolution in bins of the e-peak charge.

We have parameterize the signal arrival time and the timing resolution as functions of the e-peak size (charge).

$$f(x) = \frac{b}{x^w} + a$$

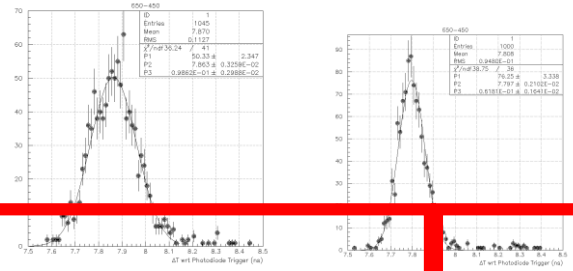

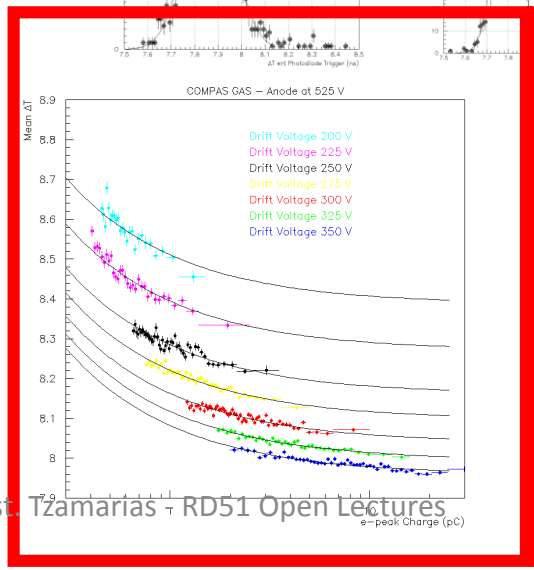

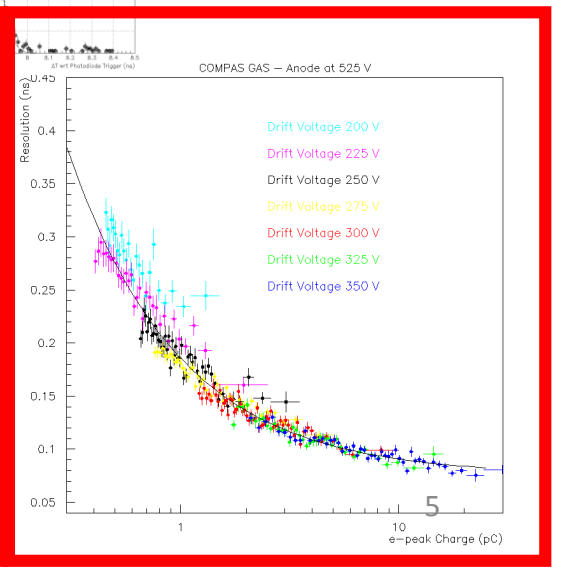

How can we combine the charge distribution parameterization (Polya) with the above timing parameterizations in order to estimate the "total" timing resolution of detector?

The signal arrival time, ΔT, distribution of a pulse with charge equal to Q is expressed as a Gaussian:

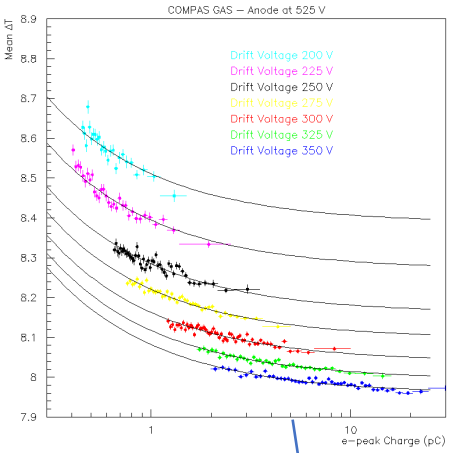

$$G\left(\Delta T; W(Q), R(Q)\right) = \frac{1}{\sqrt{2\pi}R(Q)} \exp\left(\frac{-1}{2} \cdot \left(\frac{\left(\Delta T - W(Q)\right)}{R(Q)} \right)^2 \right)$$

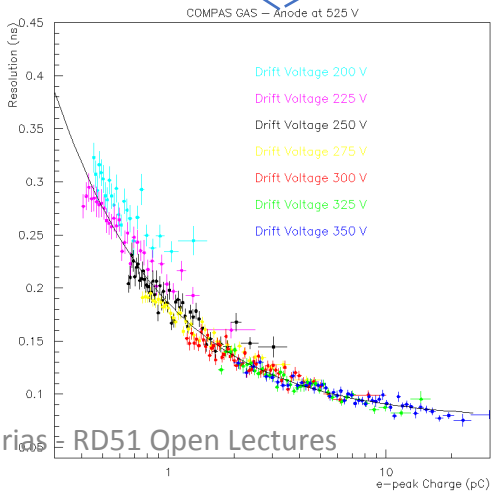

The ΔT distribution, f(ΔT), corresponding to a part of the Q spectrum, $Q \in [Q_1, Q_N]$ should be:

$$f(\Delta T) = \int_{Q_1}^{Q_N} A(Q) \cdot G(\Delta T; W(Q), R(Q)) dQ \quad (3)$$

where A(Q) is the Polya function estimated by fitting the "visible" charge distribution

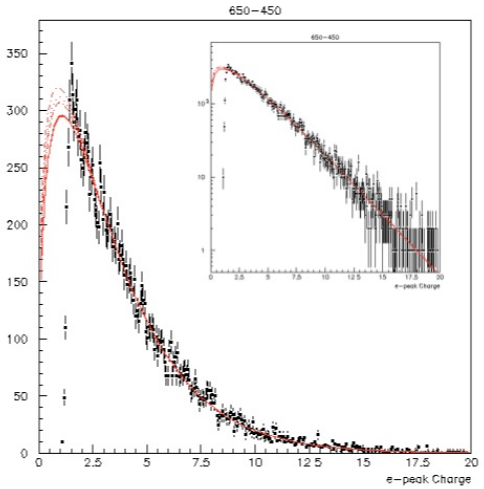

$$f(\Delta T) = \int_{Q_1}^{Q_N} A(Q) \cdot G(\Delta T; W(Q), R(Q)) dQ \quad (3)$$

Eq. 3 is aproximated as:

$$f(\Delta T) = \lim_{N \to \infty} \sum_{i=1}^{N} A(Q_i) \cdot G(\Delta T; W(Q_i), R(Q_i)) \cdot \Delta Q$$

$$\simeq \sum_{i=1}^{N_{large}} A(Q_i) \cdot G(\Delta T; W(Q_i), R(Q_i)) \, \Delta Q \qquad (4)$$

$$= \sum_{i=1}^{N_{large}} a_i \cdot g_i(\Delta T)$$

where

$$a_i = A(Q_i) \cdot \Delta Q \quad and \quad \sum_{i=1}^{N_{large}} a_i = 1 \qquad (5)$$

$$g_i(\Delta T) = G(\Delta T; W(Q_i), R(Q_i))$$

Eq. 4 expresses the distribution of ΔT as a weighted sum of Gaussian distributions with different means ($\mu_i = W(Q_i)$, $i = 1,23,\ldots N_{large}$) and variances ($V_i = R^2(Q_i)$, $i = 1,23,\ldots N_{large}$)

In many problems the Probability Distribution Function can be approximated as weighted sum of Gaussian functions.

(

We do not have to assume that the distributions are Gaussian…

Let the random variable x (e.g. the arrival time of the pico-micromegas e-peak, responding to a single photon, with respect to the photon emission time) be distributed according to the probability distribution function (pdf) f(x). Let us assume that f(x) can be expressed linearly as a sum of distributions:

$$f(x)=\sum_{i=1}^{N} a_i g_i(x) \quad where \quad \sum_{i=1}^{N} a_i = 1 \quad and \quad \int_{-\infty}^{\infty} g_i(x)dx = 1 \;\forall i$$

$$\langle x\rangle_i = \int_{-\infty}^{\infty} x g_i(x)dx, \quad \langle x^2\rangle_i = \int_{-\infty}^{\infty} x^2 g_i(x)dx, \quad V_i = \langle x^2\rangle_i - \left(\langle x\rangle_i\right)^2$$

(1)

The expected value and the variance of the variable x are expressed as:

$$E[x] = \int x f(x)dx = \int x\left(\sum_{i=1}^{N} a_i g_i(x)\right)dx = \sum_{i=1}^{N} a_i \int x g_i(x)dx = \sum_{i=1}^{N} a_i \langle x\rangle_i$$

$$V[x] = \int x^2 f(x)dx - \left(\int x f(x)dx\right)^2 = \sum_{i=1}^{N} a_i \langle x^2\rangle_i - \left(\sum_{i=1}^{N} a_i \langle x\rangle_i\right)^2$$

(2)

The expected value has been expressed easily as a weighted sum of the means of the g_i distributions. However some more algebra is needed to express V[x] in terms of the variances and the means of gi's .

$$V[x] = \sum_{i=1}^{N} a_i \langle x^2 \rangle_i - \left(\sum_{i=1}^{N} a_i \langle x \rangle_i \right)^2$$

$$= \sum_{i=1}^{N} a_i \left(a_i + (1 - a_i) \right) \langle x^2 \rangle_i - \sum_{i=1}^{N} a_i^2 \langle x \rangle_i^2 - \sum_{\substack{i,j=1 \\ i \neq j}} a_i a_j \langle x \rangle_i \langle x \rangle_j$$

$$= \sum_{i=1}^{N} a_i (1 - a_i) \langle x^2 \rangle_i - \sum_{\substack{i,j=1 \\ i \neq j}}^{N} a_i a_j \langle x \rangle_i \langle x \rangle_j$$

$$= \sum_{i=1}^{N} a_i^2 \left(\langle x^2 \rangle_i - \langle x \rangle_i^2 \right) + \sum_{i=1}^{N} a_i \langle x^2 \rangle_i \sum_{\substack{j=1 \\ j \neq i}}^{N} a_j - \sum_{\substack{i,j=1 \\ i \neq j}}^{N} a_i a_j \langle x \rangle_i \langle x \rangle_j$$

$$= \sum_{i=1}^{N} a_i^2 V_i + \sum_{\substack{i,j=1 \\ i \neq j}}^{N} a_i a_j \left(\langle x^2 \rangle_i - \langle x \rangle_i \langle x \rangle_j \right) = \sum_{i=1}^{N} a_i^2 V_i + \sum_{\substack{i=1 \\ j=i+1}}^{N} a_i a_j \left(\langle x^2 \rangle_i + \langle x^2 \rangle_j - 2 \langle x \rangle_i \langle x \rangle_j \right)$$

$$= \sum_{i=1}^{N} a_i^2 V_i + \sum_{\substack{i=1 \\ j=i+1}}^{N} a_i a_j \left(V_i + V_j + \langle x \rangle_i^2 + \langle x \rangle_j^2 - 2 \langle x \rangle_i \langle x \rangle_j \right) = \sum_{i=1}^{N} a_i^2 V_i + \sum_{\substack{i=1 \\ j=i+1}}^{N} a_i a_j \left(V_i + V_j + \left(\langle x \rangle_i - \langle x \rangle_j \right)^2 \right)$$

(3)

In case that the g_i distributions have the same mean values then eq. 3 can be simplified to:

$$V[x] = \sum_{i=1}^{N} a_i^2 V_i + \sum_{\substack{i=1 \\ j=i+1}}^{N} a_i \; a_j \; (V_i + V_j) = \sum_{i=1}^{N} a_i^2 V_i + \sum_{\substack{i=1 \\ j=1 \\ j \neq i}}^{N} a_i \; a_j \; V_i$$

$$= \sum_{i=1}^{N} a_i \; V_i \left(a_i + \sum_{\substack{j=1 \\ j \neq i}}^{N} a_i \right) = \sum_{i=1}^{N} a_i \; V_i \qquad (4)$$

)

$$E[\Delta T] = \sum_{i=1}^{N_{large}} a_i \cdot \mu_i$$

$$V[\Delta T] = \sum_{i=1}^{N_{large}} a_i^2 \cdot V_i + \sum_{i=1}^{N_{large}} a_i \cdot a_j \left(V_i + V_j + \left(\mu_i - \mu_j \right)^2 \right) \quad (6)$$

$i \rightarrow Q_i \in [Q_1, Q_2]$

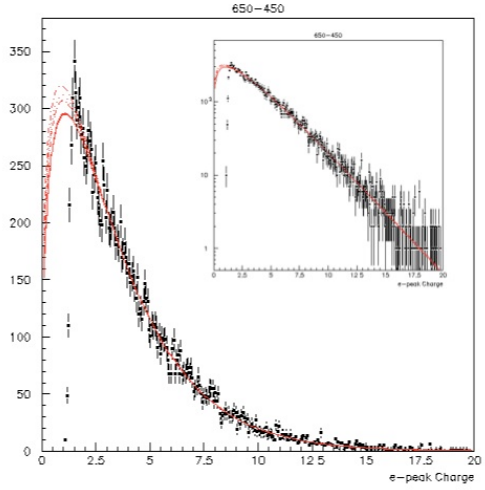

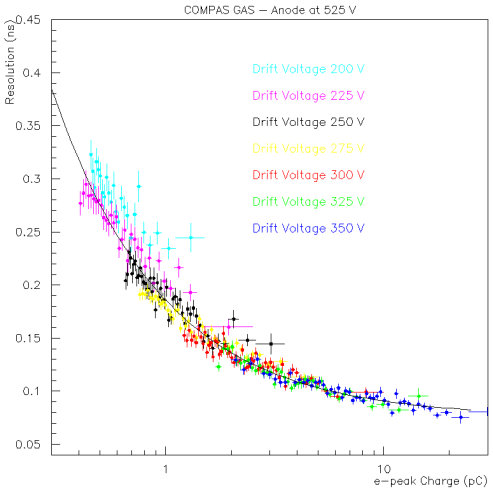

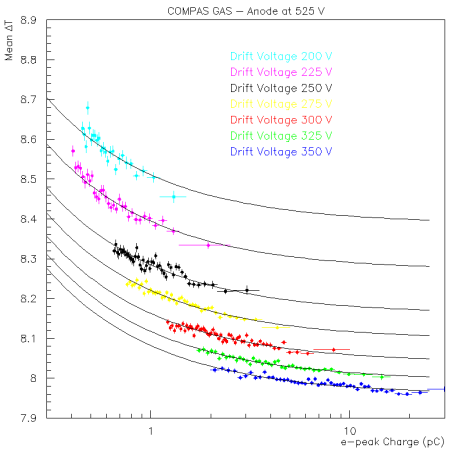

$\alpha_i = P_{pe}(Q_i)$ $V_i = \{R(Q_i)\}^2$ $\mu_i = \{W(Q_i)\}^2$

The statistical error of the convolution is given by propagating the the parameterization errors

$$\delta_{V[\Delta T]} = \left[\sum_{i=1}^{N_{large}} a_i \cdot \delta_i^2 + 4 \sum_{i=1}^{N_{large}} a_i^2 \cdot \left(\mu_i - \sum_{j=1}^{N_{large}} a_j \cdot \mu_j \right)^2 w_i^2 \right]^{1/2} \quad (7)$$

Global, Single p.e. Timing Resolution ($V_{e\text{-}peak}$ > 0.01 V) as a function of the applied drift voltage, for different anode voltages.

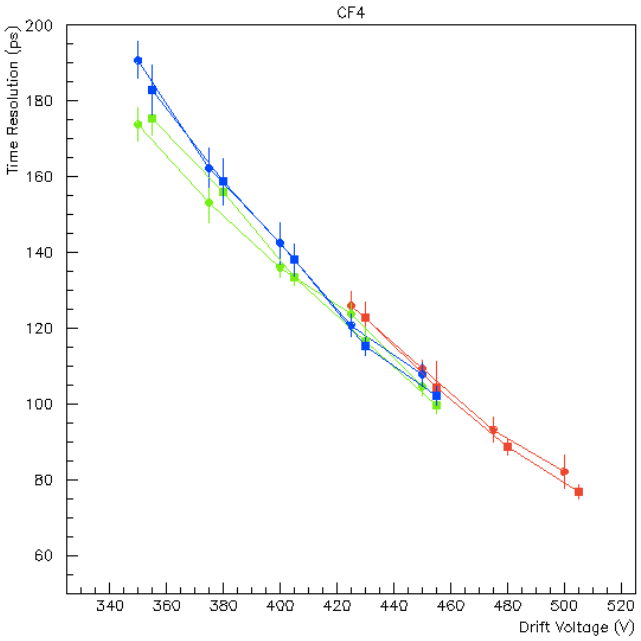

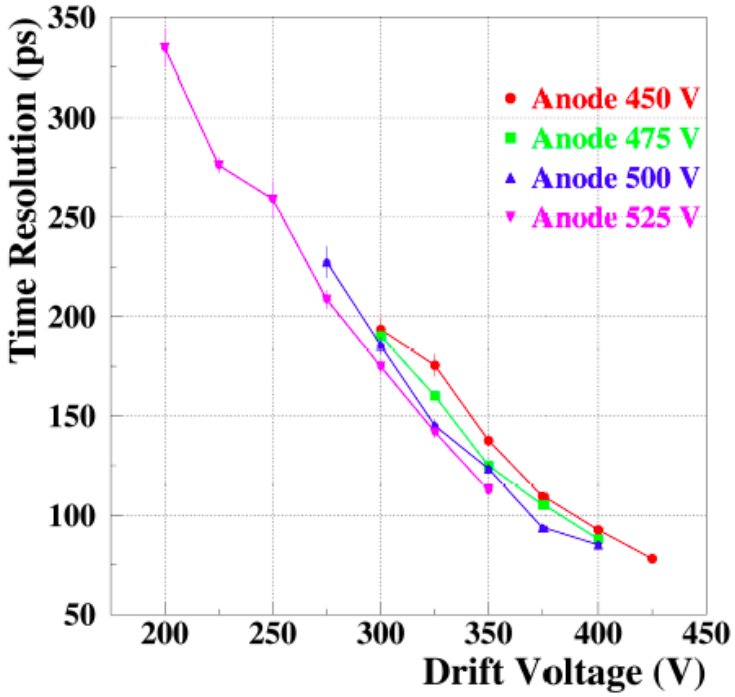

Figure 10: Laser test: Dependence of the corrected time resolution with the drift voltage for anode voltages of 450 V (red circles), 475 V (green squares), 500 V (blue triangles) and 525 V (magenta inverted triangles). Statistical uncertainties are shown.

Statistical properties of the convolution

Table - 9

COMPASS Resolution based on e-Peak Amplitude

Anode Voltage (V)	Drift Voltage (V)	Experimental Measurements: Analysis Threshold (V)	Experimental Measurements: Raw Resolution (ps)		Experimental Measurements: Slewing Corr. Resolution (ps)		Convolution up to the Analysis Threshold: Raw Resolution (ps)		Convolution up to the Analysis Threshold: Slewing Corr. Resolution (ps)		Predicted Resolution (e-Peak Amplitude > 0.01 V): Raw Resolution (ps)		Predicted Resolution (e-Peak Amplitude > 0.01 V): Slewing Corr. Resolution (ps)		Scaled Experimental Resolutions (e-Peak Amplitude > 0.01 V): Raw Resolution (ps)		Scaled Experimental Resolutions (e-Peak Amplitude > 0.01 V): Slewing Corr. Resolution (ps)	
	300	0.016	166.2	±6.0	165.2	±6.0	159.3	±1.5	158.3	±1.1	216.0	±5.0	211.5	±3	225.4	±11.3	220.7	±10.2
	325	0.018	144.2	±3.1	143.6	±2.5	144.2	±0.7	142.1	±0.5	190.8	±2.2	183.0	±1.6	190.8	±6.5	184.0	±5.7
	350	0.02	120.7	±1.7	119.5	±1.4	123.2	±0.7	121	±0.5	160.2	±3.0	151	±1.5	156.9	±5.2	149.1	±3.7
	375	0.035	88.6	±0.9	88.8	±0.7	89.5	±0.5	88.7	±0.5	122.4	±12.5	114.3	±9.5	121.2	±12.9	114.4	±9.9
	400	0.05	77.1	±0.4	78	±0.7	77.6	±0.4	77.2	±0.3	97.4	±7.7	92.3	±5.6	96.8	±7.9	93.3	± 5.9
450	425	0.1	70.8	±0.9	70.8	±0.6	69.3	±0.3	69.2	±0.3	78.7	±3.7	76.7	±2.7	80.4	±4.0	78.5	±2.9
	300	0.0125	184.8	±2.4	184.3	±2.3	194.1	±1	190	±0.5	211.8	±7	205.13	±6	201.7	±7.4	199.0	±6.5
	325	0.017	139	±3.3	139	±1.4	145	±0.6	141.6	±0.5	171.6	±10	163	±8	164.5	±10.7	160.0	±8.3
	350	0.034	100.6	±0.6	100.1	±0.6	101.1	±0.5	100	±0.4	136.4	±13.3	127.8	±10.2	135.7	±13.7	127.9	±10.6
	375	0.035	90	±0.7	91	±0.7	92	±0.5	90.7	±0.3	112.5	±7.9	105.9	±0.6	110.1	±8.0	106.3	±1.8
475	400	0.05	79.1	±0.5	80.5	±0.5	79.4	±0.4	78.7	±0.2	91.1	±4.7	87.4	±3.3	90.8	±4.9	89.4	±3.5
	275	0.022	179.3	±3.1	180.7	±1.2	183.5	±1	180.8	±0.8	242.7	±22.2	231.4	±18.8	237.1	±22.8	231.3	±19.5
	300	0.025	151.9	±4.1	153.2	±1.3	158.6	±0.7	155.3	±0.8	207.9	±18.4	194.7	±14.6	199.1	±19.0	192.1	± 15.0
	325	0.034	117.6	±3.5	118.8	±0.8	121.8	±0.7	119	±0.5	164.8	±16.3	150.6	±11.7	159.1	±17.0	150.3	±12.1
	350	0.05	99.5	±1.5	100.6	±0.5	102	±0.5	100.3	±0.3	132.3	±11.6	121.6	±8	129.1	±11.9	122.0	±8.3
	375	0.1	87.5	±0.5	88.2	±0.8	86.7	±0.4	86.2	±0.3	101	±5.6	96.6	±4	101.9	±5.9	98.8	±4.3
500	400	0.12	80.1	±0.5	80.8	±1.2	79.6	±0.3	79.1	±0.3	87.4	±3.2	84.7	±2.2	87.9	±3.4	86.5	±2.7
	200	0.012	330.3	±3.5	326.1	±3.5	325.2	±2.1	321.9	±2.0	358.8	±13.8	354.1	±13.3	364.4	±14.9	358.7	±13.9
	225	0.013	279.8	±3.7	281.8	±8.8	282.1	±1.1	278	±1.1	321.3	±15.2	314.7	±14.2	318.7	±16.1	319.0	±17.9
	250	0.018	218.1	±3.6	202.8	±4.5	211.6	±1	208.8	±1	278.1	±24.7	269	±22.6	286.6	±26.8	261.3	±23.4
	275	0.018	175.2	±3.5	176.3	±3.3	185.5	±1.0	180.2	±0.7	234.4	±18.4	222.4	±15.7	221.4	±18.5	217.6	±16.4
	300	0.035	133.3	±1.5	133.7	±1.0	135.8	±0.8	133.8	±0.8	194.5	±21.7	182.8	±18	190.9	±22.1	182.7	±18.7
	325	0.048	111.7	±1.1	112.5	±1.0	113.8	±0.6	112.2	±0.4	157	±16	146.3	±12.7	154.1	±16.3	146.7	±13.2
525	350	0.05	100.9	±0.8	102.3	±0.7	101.9	±0.5	100.5	±0.5	118.2	±6.4	112.2	±4.5	117.0	±6.6	114.2	±4.8

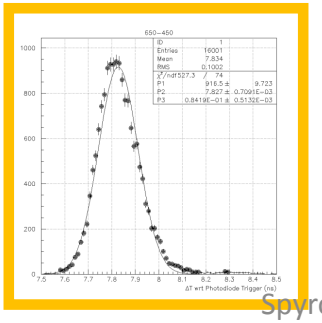

Statistical properties of the convolution

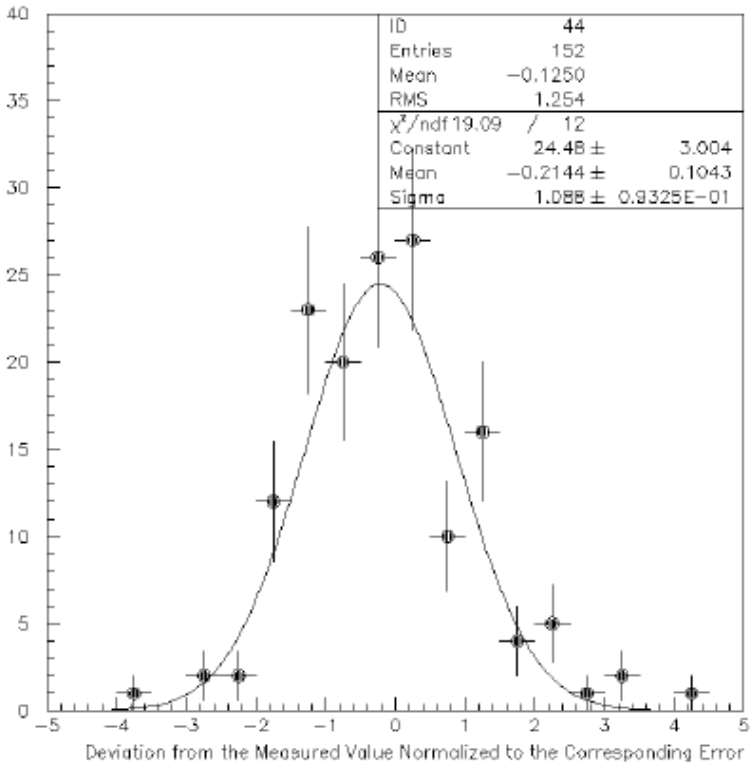

Figure 21 *: The distribution of the difference between the calculated resolutions and the related experimental measurements, normalized to the statistical errors. The data points correspond to all the data sets tabulated in Tables 7-10. The solid curve represents Gaussian fit to the data points.*

Use timing to examine charge properties and use charge to combine timing measurements

MCP: The time reference devise

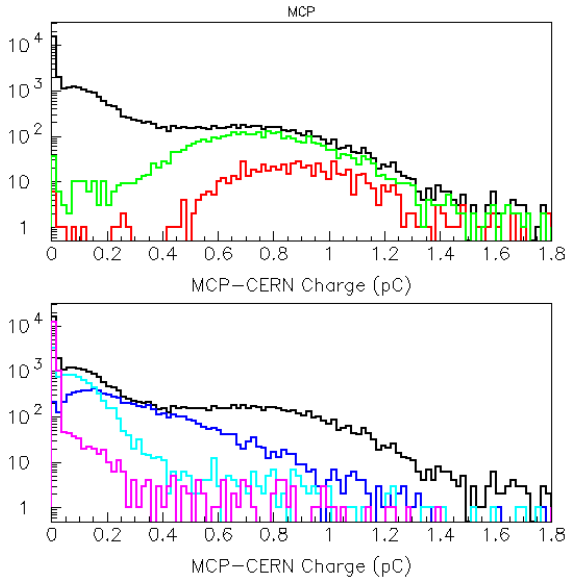

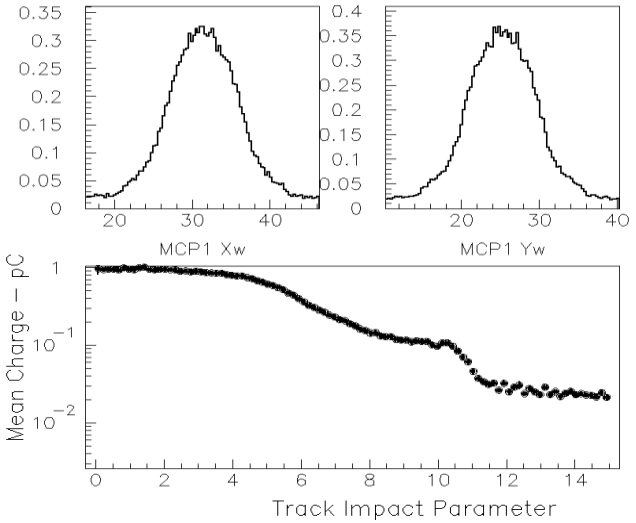

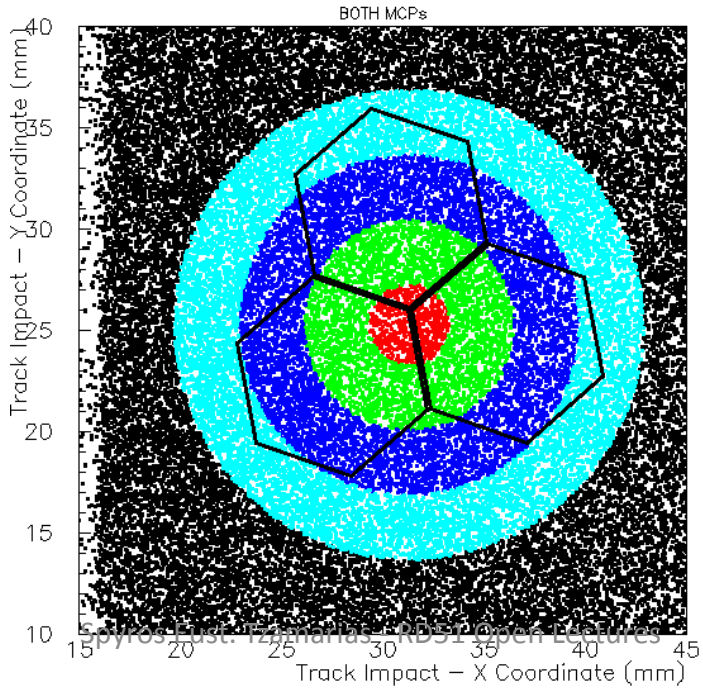

The PICOSEC PADs

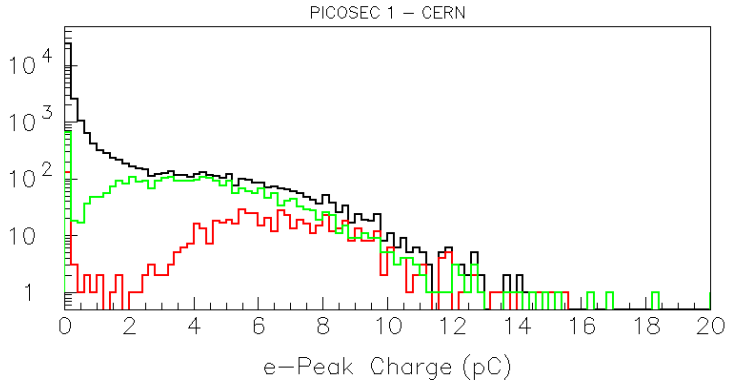

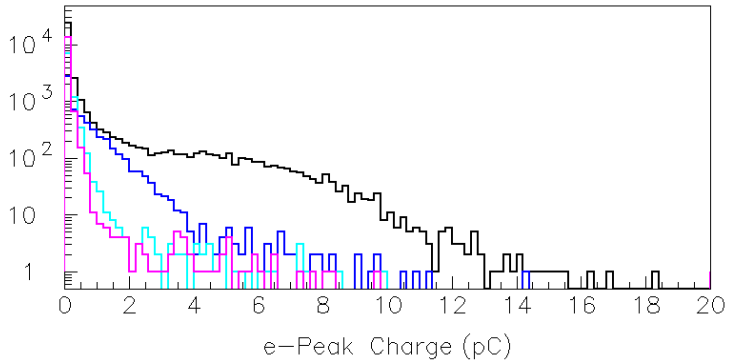

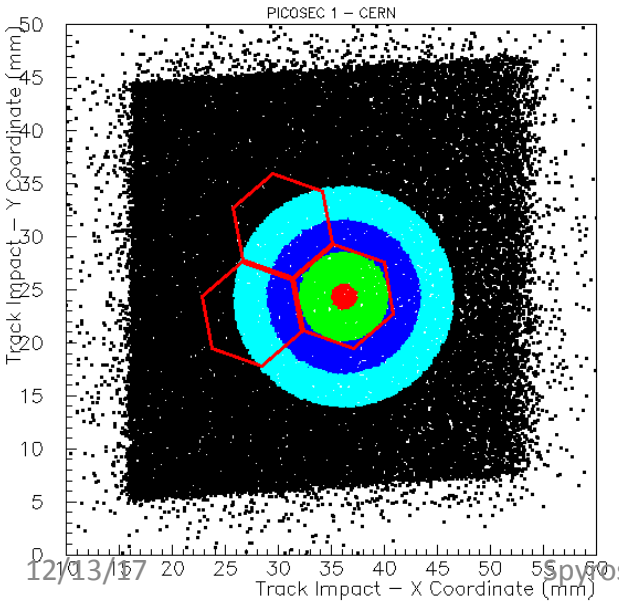

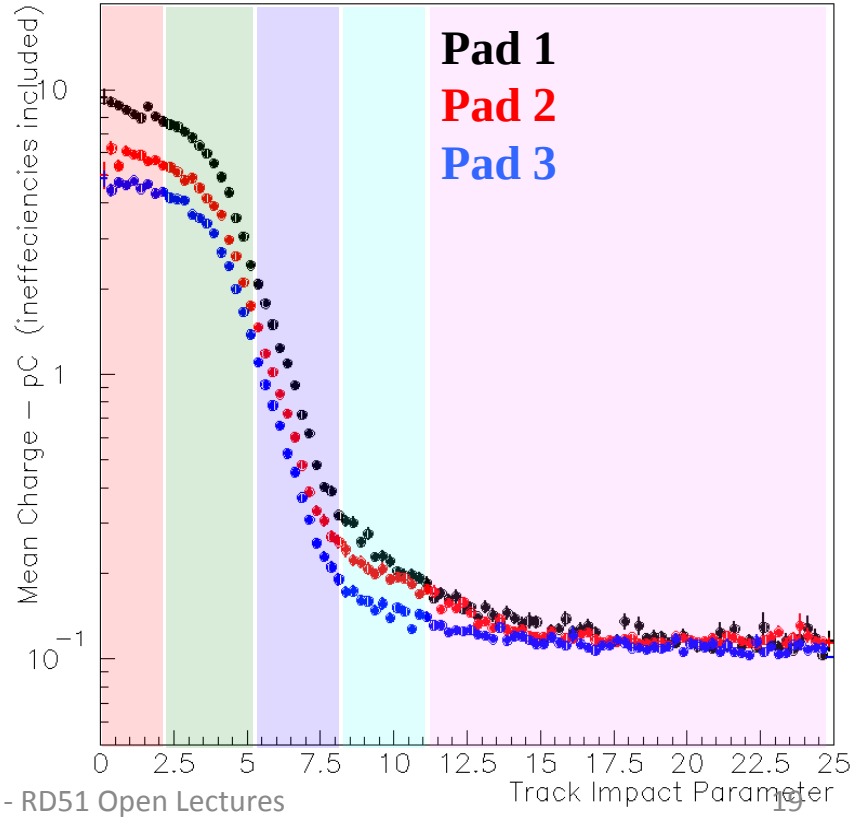

Charge Distributions

Anode area
Track Impact Parameter < 5mm

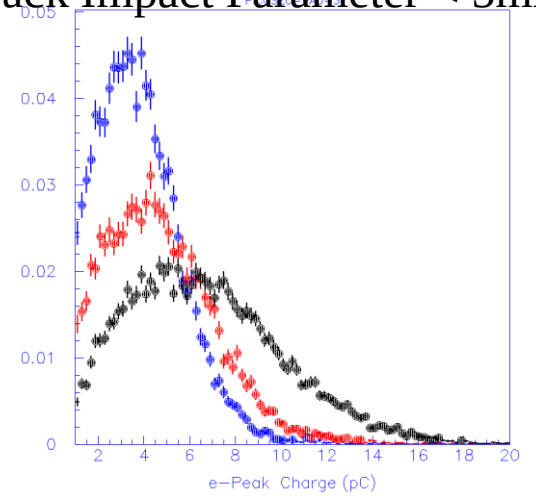

Inner Ring:Track Impact Parameter < 2mm

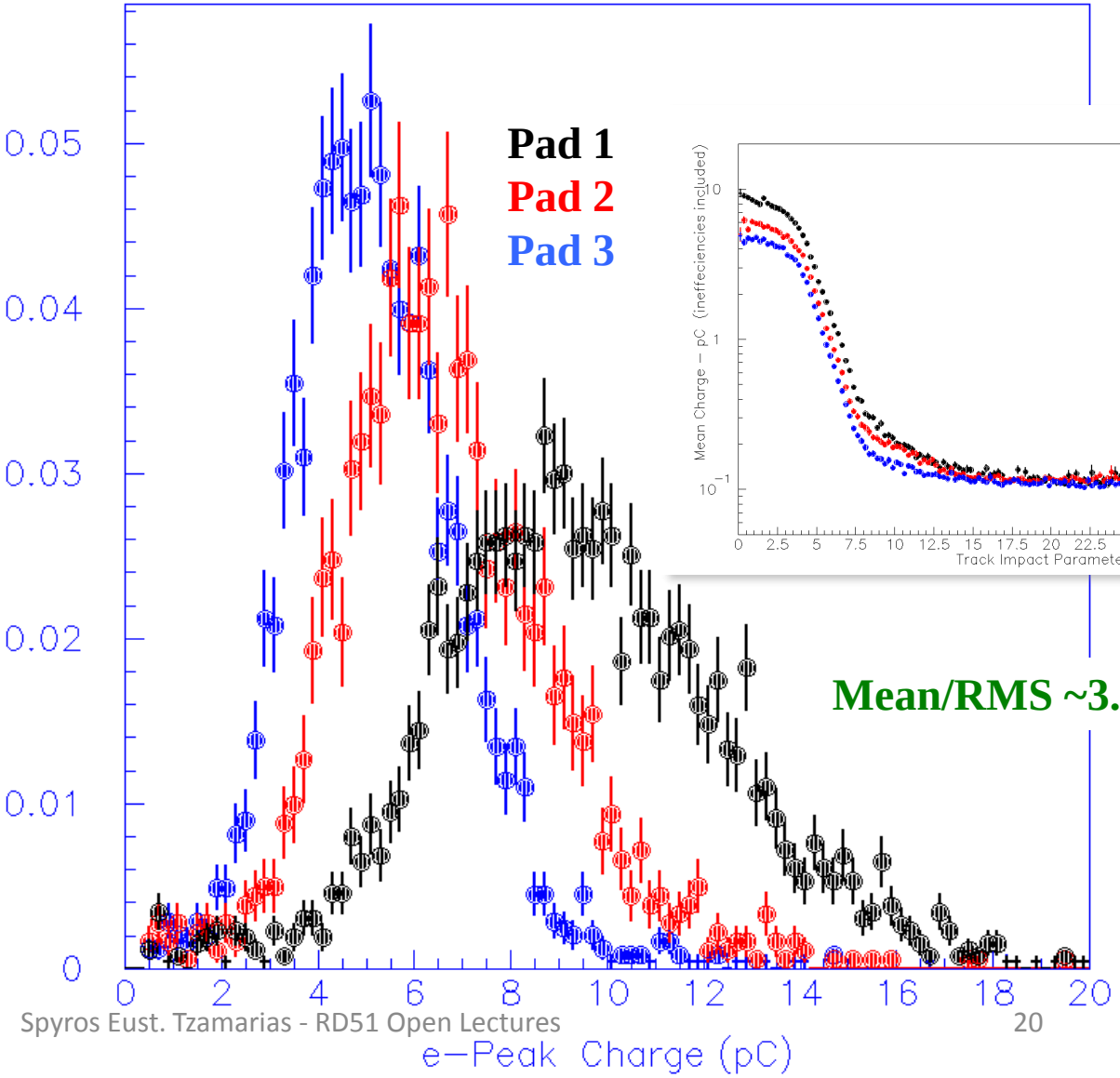

Assuming that the different PADs "charge scales" are due to external electronic gains, we could equalize the charge distributions …

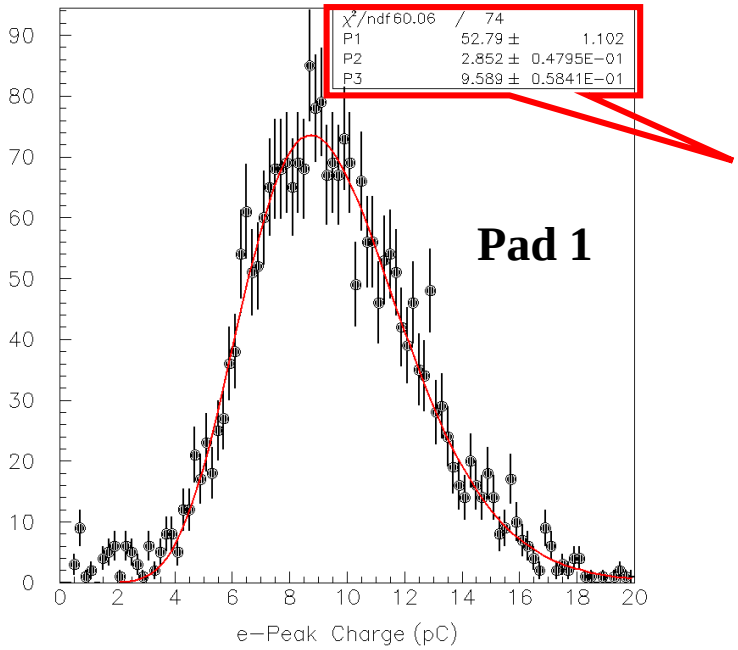

Polya Fit:
P1: RMS
P2: Mean Charge

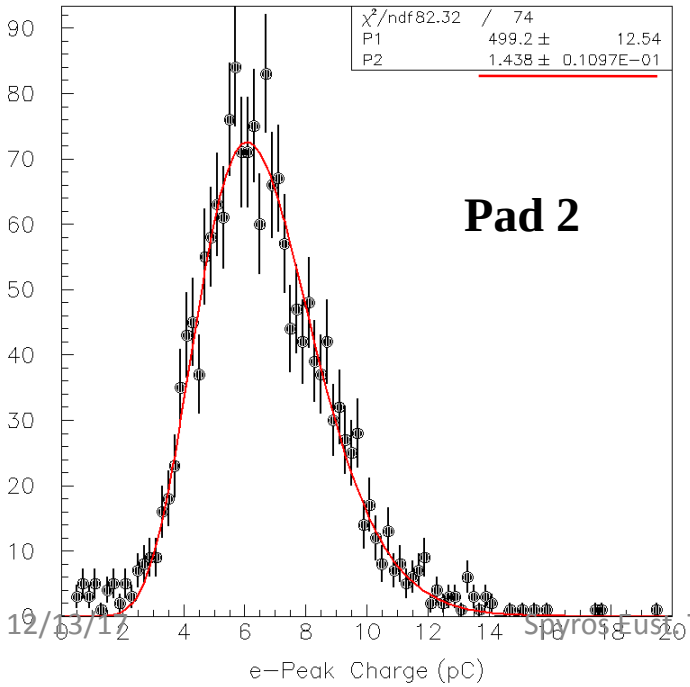

Scaling Factors

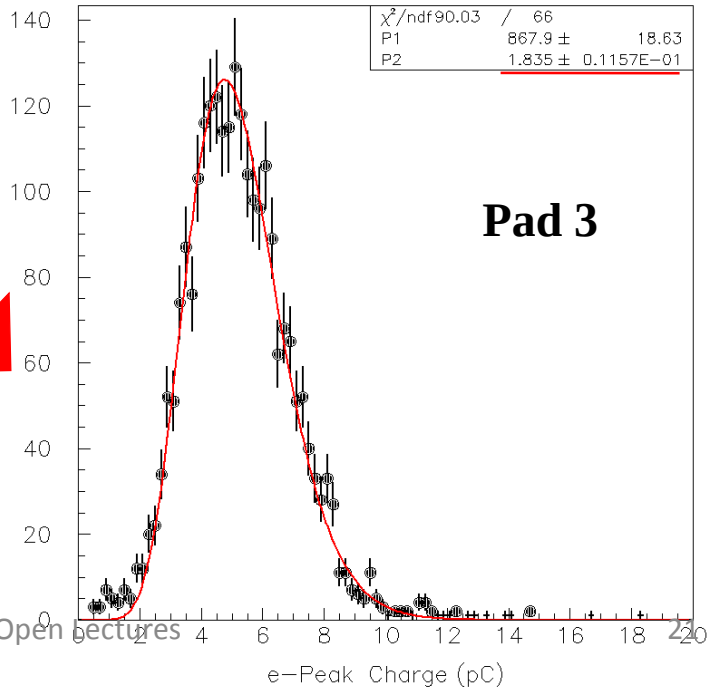

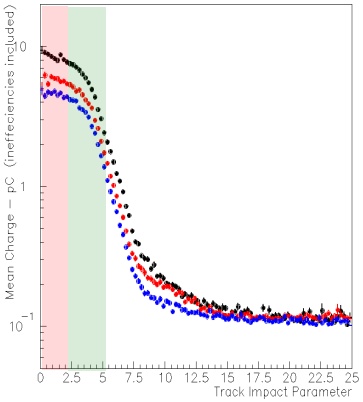

Gain Equalization (?)

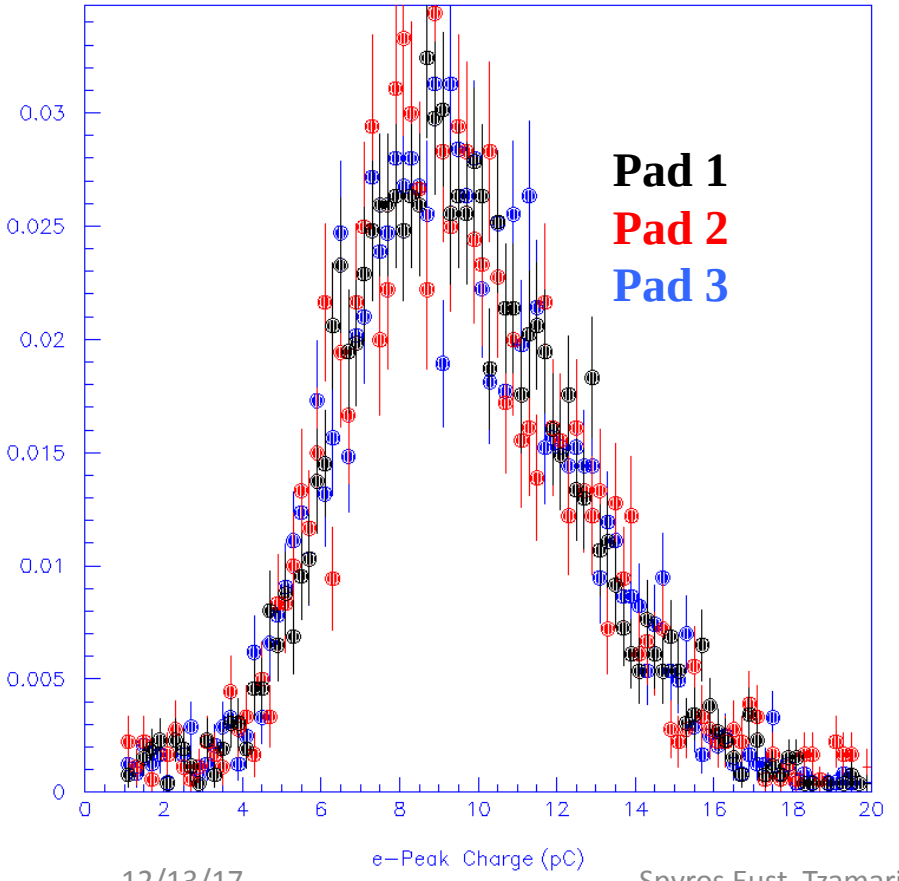

Tracks within the PAD's inner ring

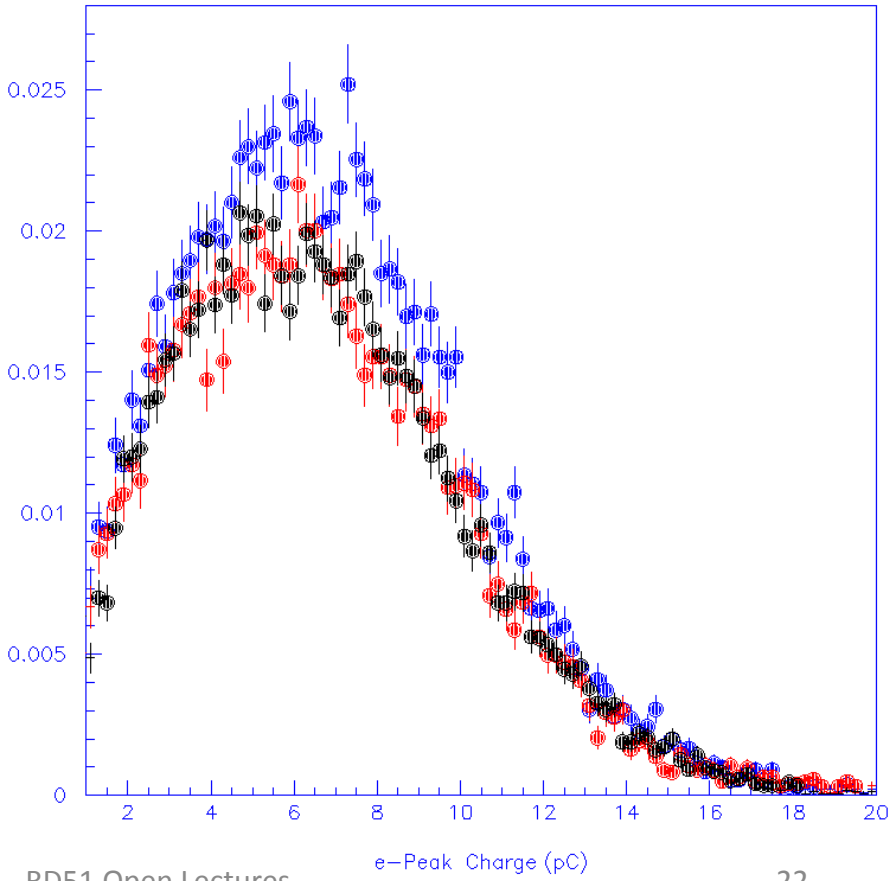

Tracks within the PAD's anode area

PRELIMINARY

PICOSEC Single PAD Time Resolution

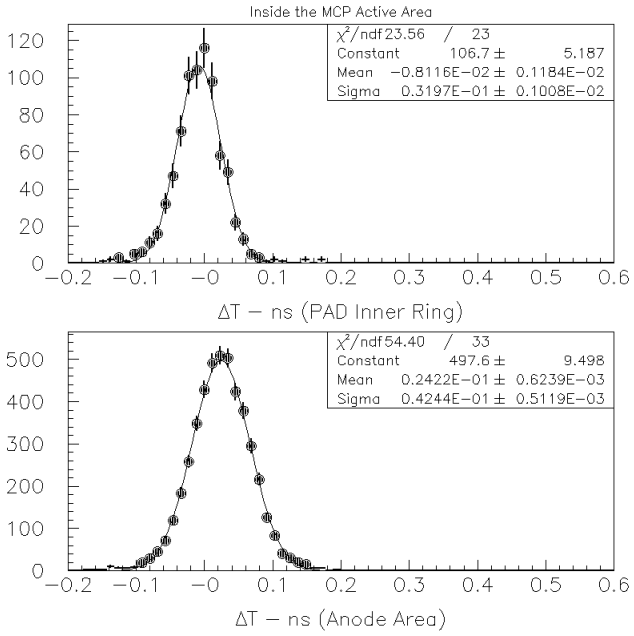

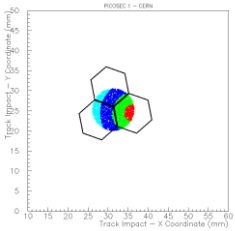

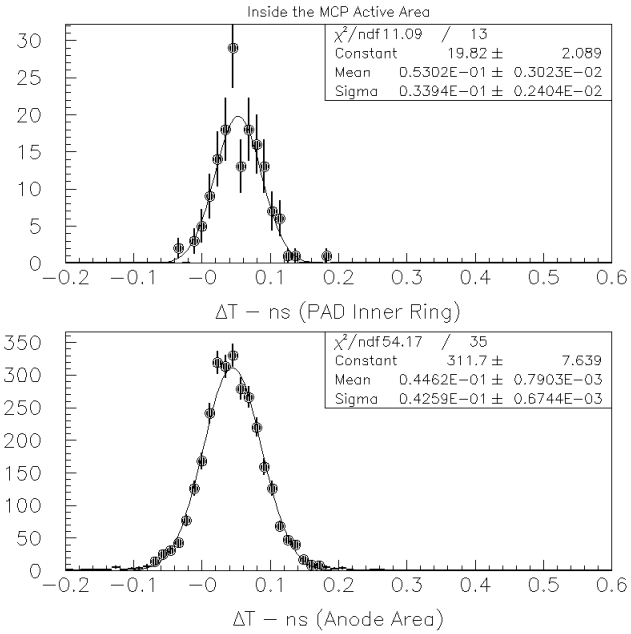

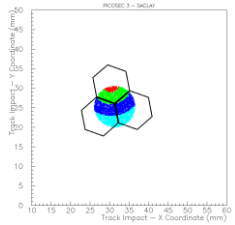

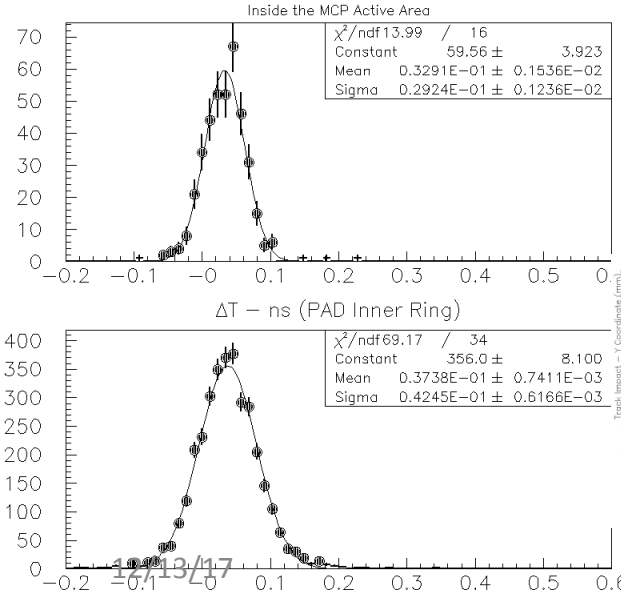

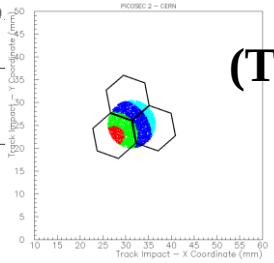

Timing Resolution

using tracks within the MCP "active area" and passing through the PICOSEC-PAD central region

~32 ps

(Tracks inside the anode area: ~42.5 ps)

Use the timing characteristics to check the charge scaling

Estimate the mean signal arrival time and the timing resolutions in bins of the e-peak charge

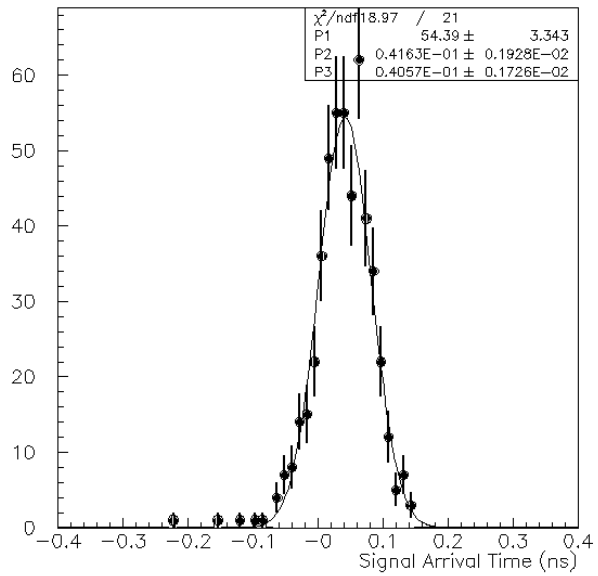

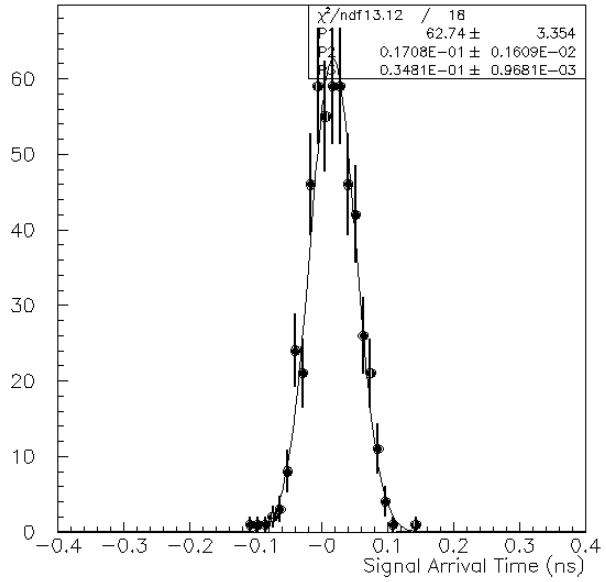

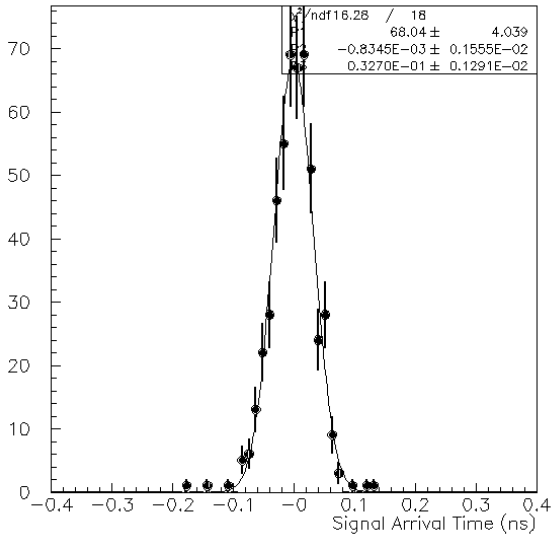

Evaluate the dependence of the mean arrival time and the timing resolution on the e-peak size, using the raw and the scaled charge.

The scaling, introduced to "equalize" the charge distributions, results to non-uniform timing characteristics !!!

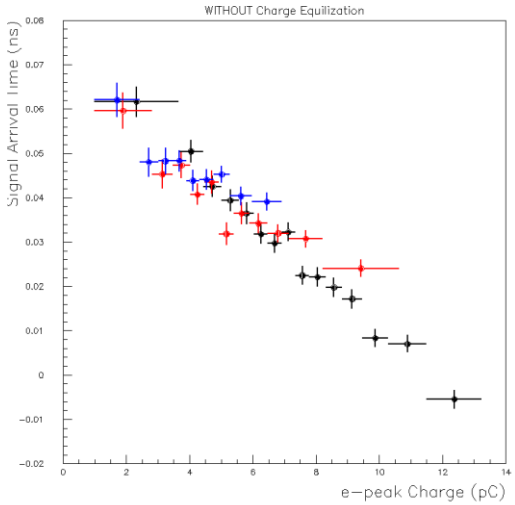

Raw Charge

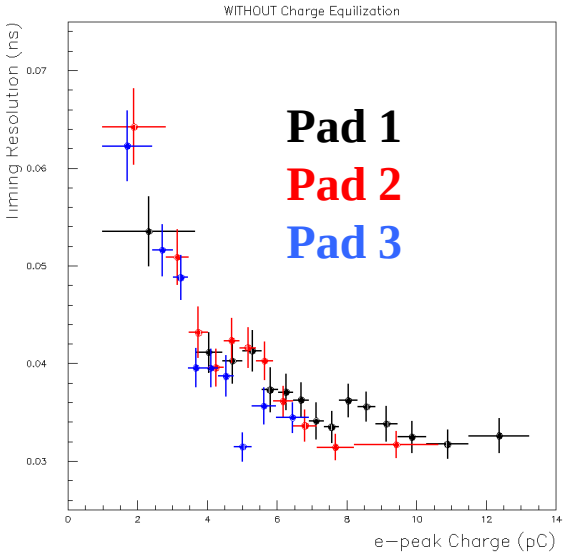

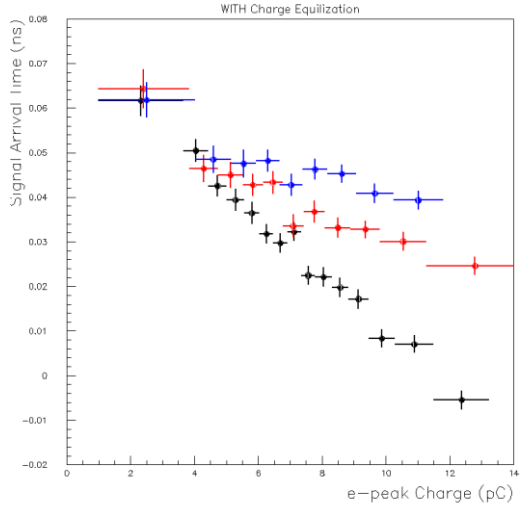

Scaled Charge

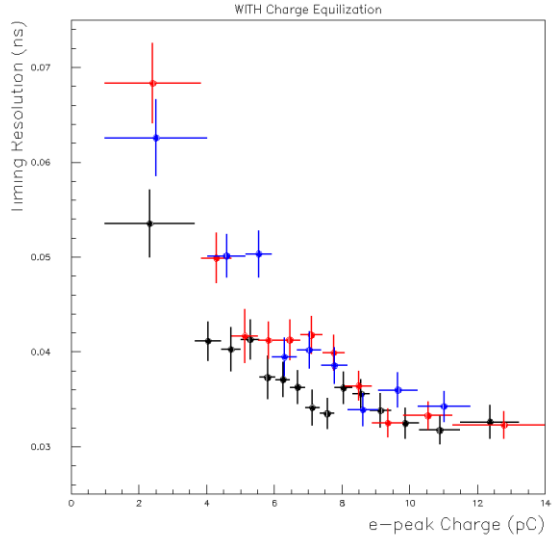

The observed difference in the charge distributions could result either from photocathode inhomogeneities or from drift field distortions or….

Correct the SAT estimations for dependences on the e-peak charge, synchronize pads (constant relative delays) and treat all the pad signals together. Check the pull distributions.

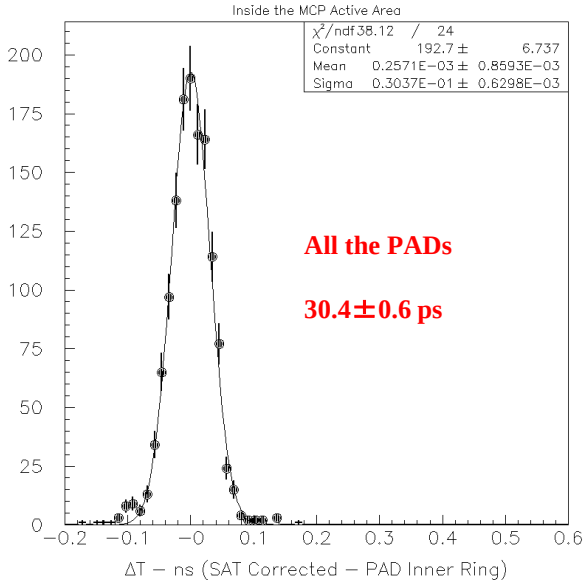

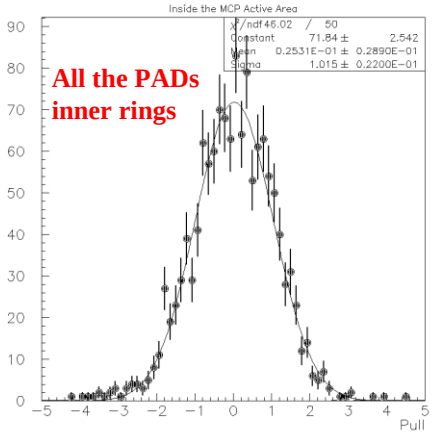

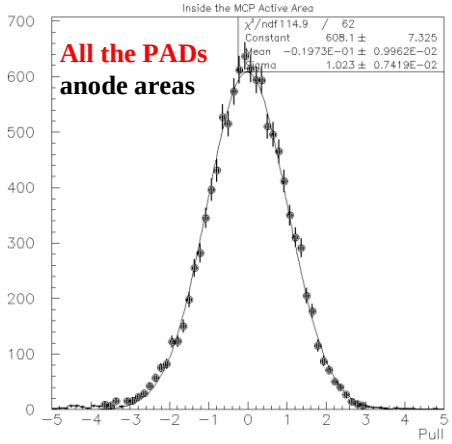

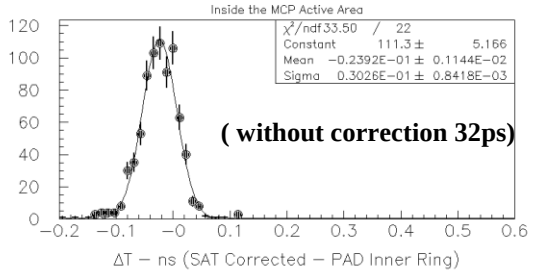

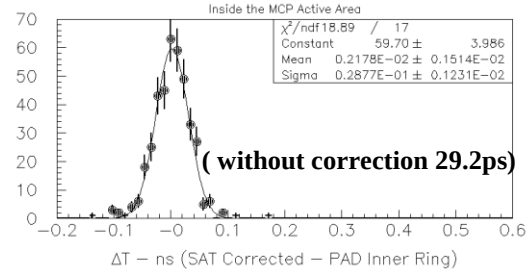

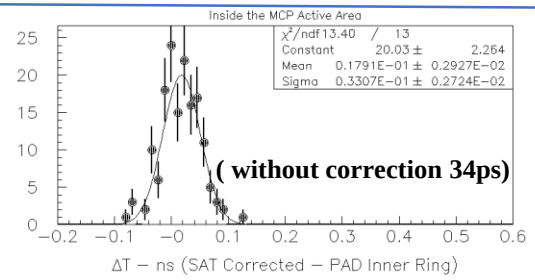

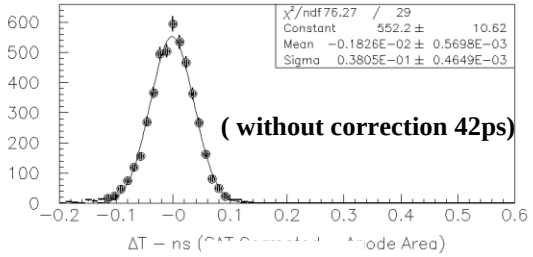

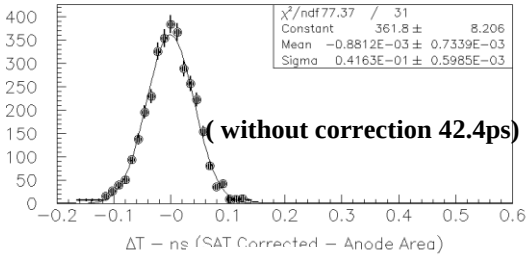

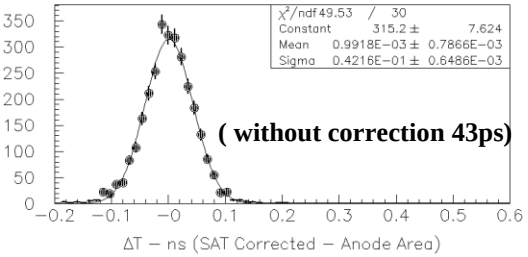

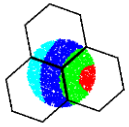

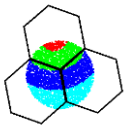

Combine the timing information from adjacent PADs
A simple exercise

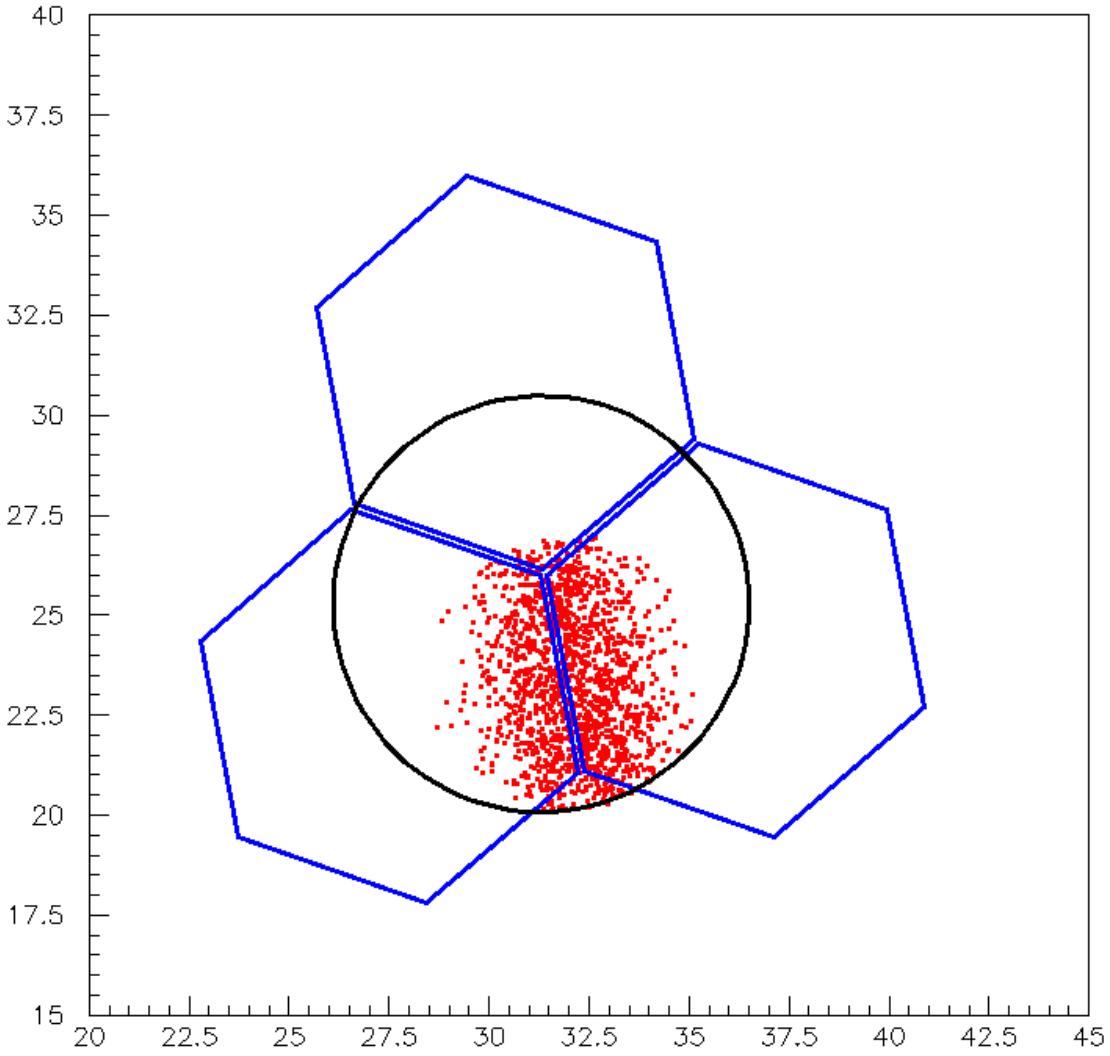

- **Concentrate on tracks with impact points in the area between PADs 1 and 2**
- **Estimate the muon arrival time using the e-peak signal of each PAD (single PAD timing).**
- **Use the parameterizations, expressing the timing resolution and SAT as functions of the e-peak charge, to combine the two timing estimations**

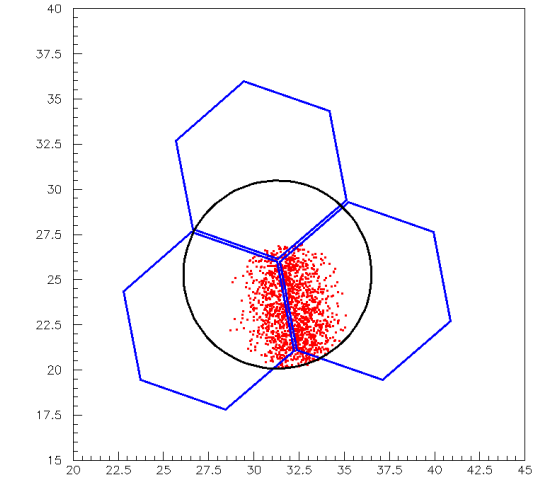

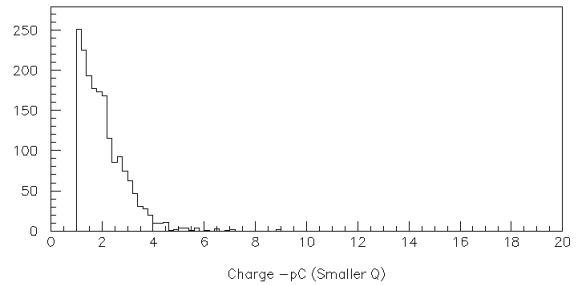

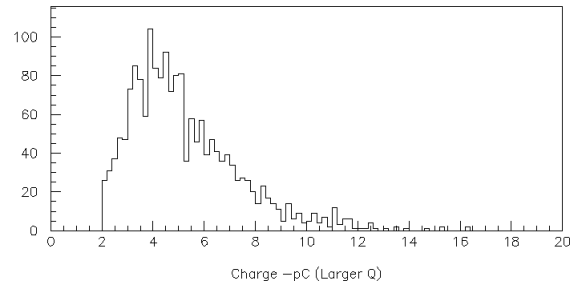

Use SAT vs Q
To "synchronize" e-peaks with different charge

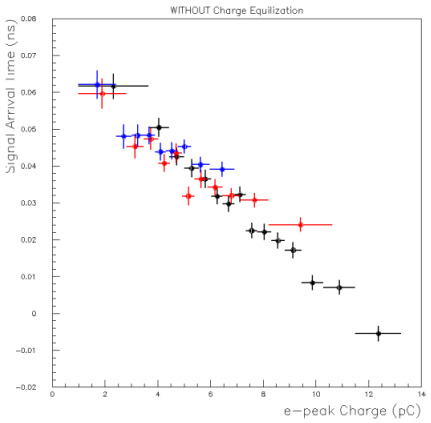

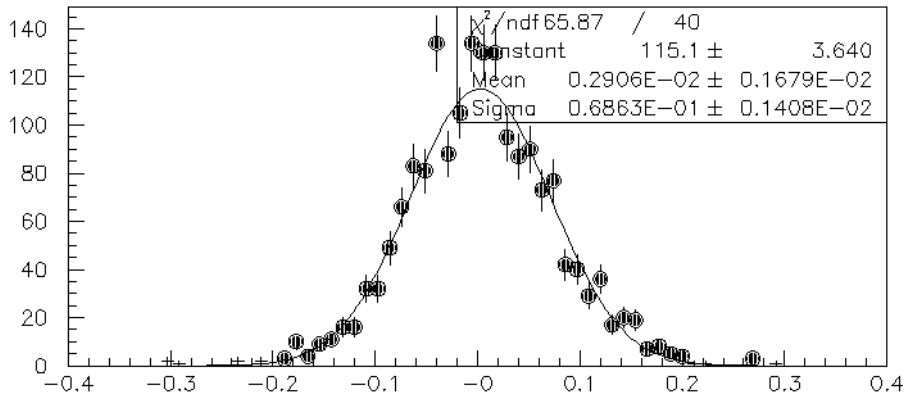

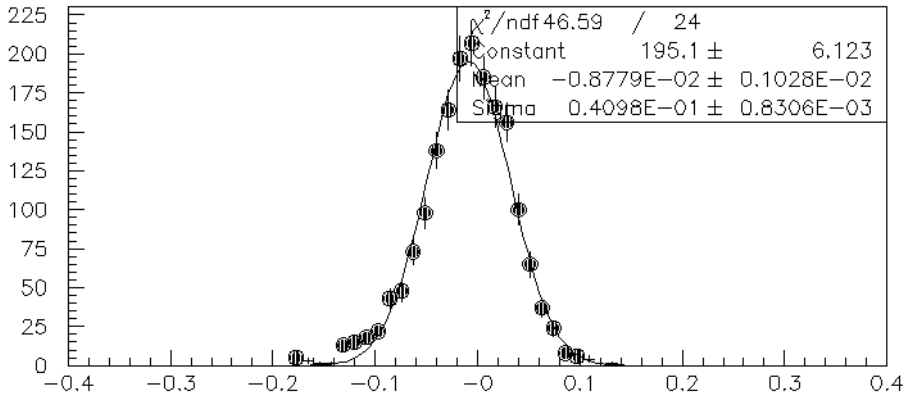

Naturally, neither of the pads achieves the optimum timing resolution, i.e. the timing resolution when all the produced photoelectrons are detected by the same pad

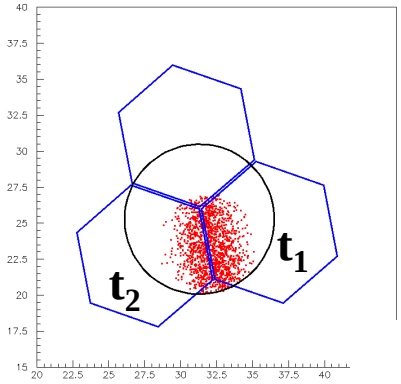

$$\chi^2 = \sum_{i=1}^{2} \frac{\left(\hat{t} - t_i + W(Q_i)\right)^2}{\left(R(Q_i)\right)^2}$$

$$\hat{t} = \frac{\sum_{i=1}^{2} \frac{\left(t_i + W(Q_i)\right)}{\left(R(Q_i)\right)^2}}{\sum_{i=1}^{2} \frac{1}{\left(R(Q_i)\right)^2}}$$

$$\delta_{\hat{t}} = \sqrt{\frac{1}{\sum_{i=1}^{2} \frac{1}{\left(R(Q_i)\right)^2}}}$$

W(Q)

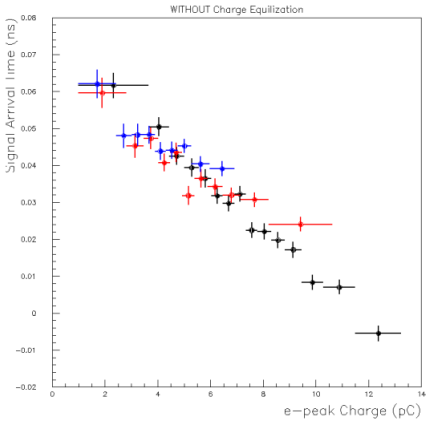

R(Q)

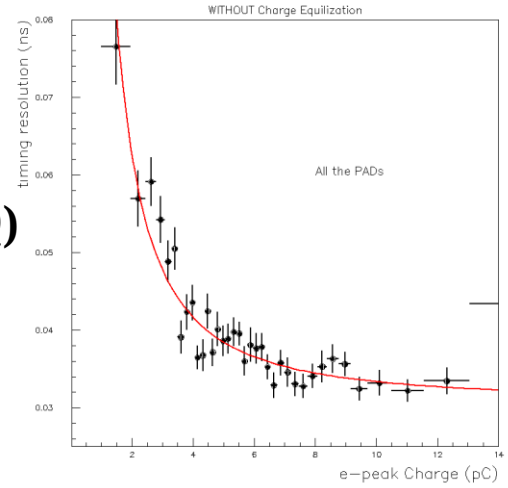

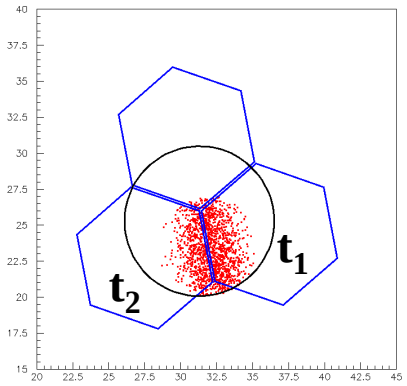

The weighted average of the two timing information almost recovers the optimum timing resolution

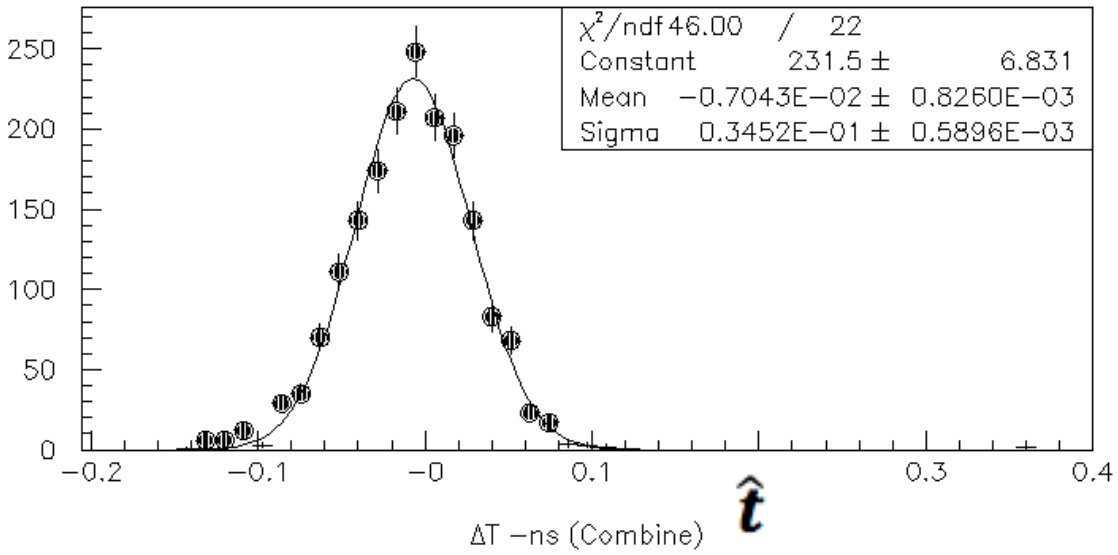

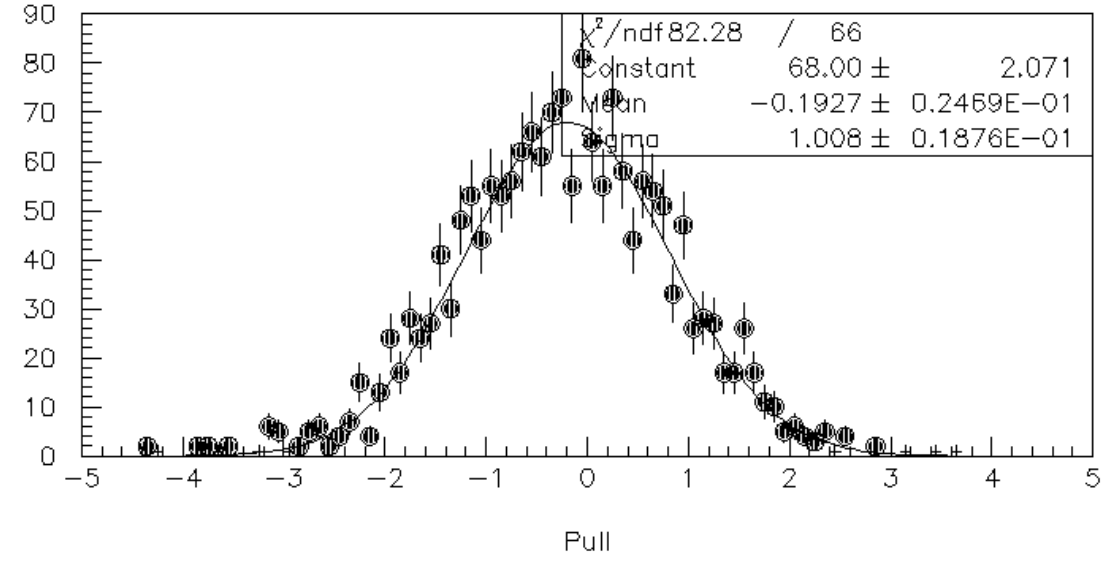

The last example
Response to a Single Photoelectron

The signal arrival time dependents on the e-peak size, following the same functional form where b and w does not depend on the drift voltage.

$$f(x) = \frac{b}{x^w} + a$$

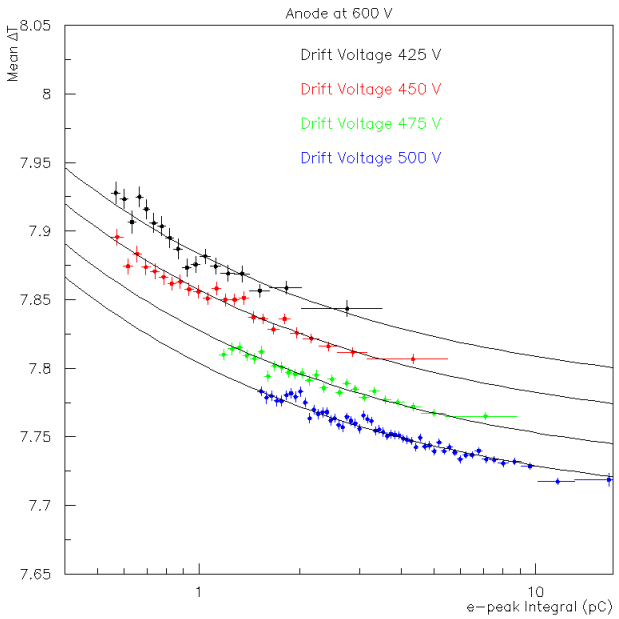

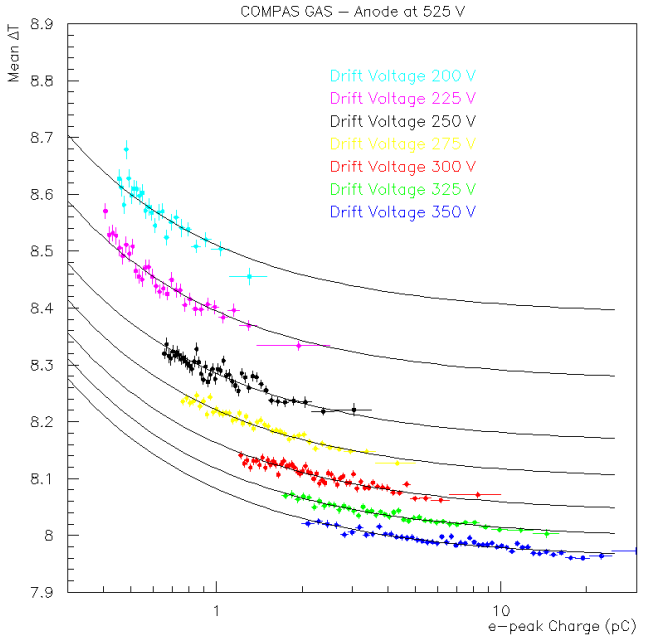

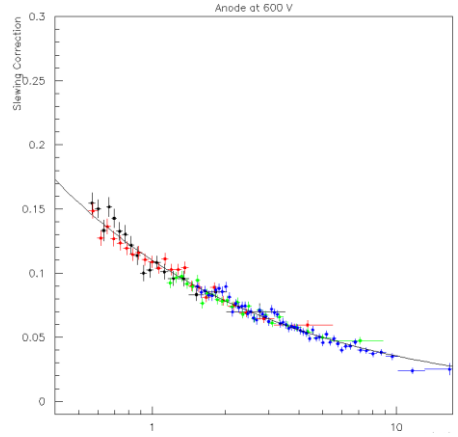

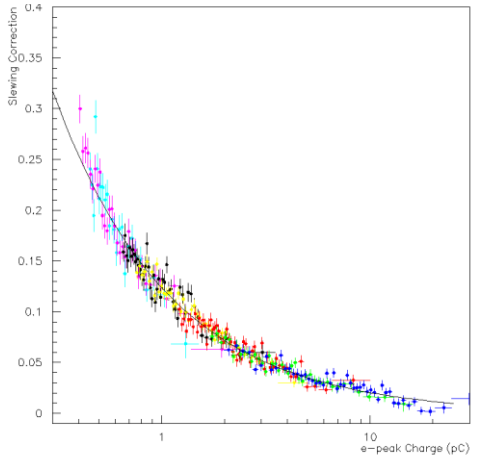

$CF_4+20\%C_2H_6$ at 0.5 bar

"Compass gas" $(Ne+10\%C_2H_6+10\%CF_4)$ at 1 bar.

The time resolution dependence on the e-peak size follows the same function, independently of the drift voltage

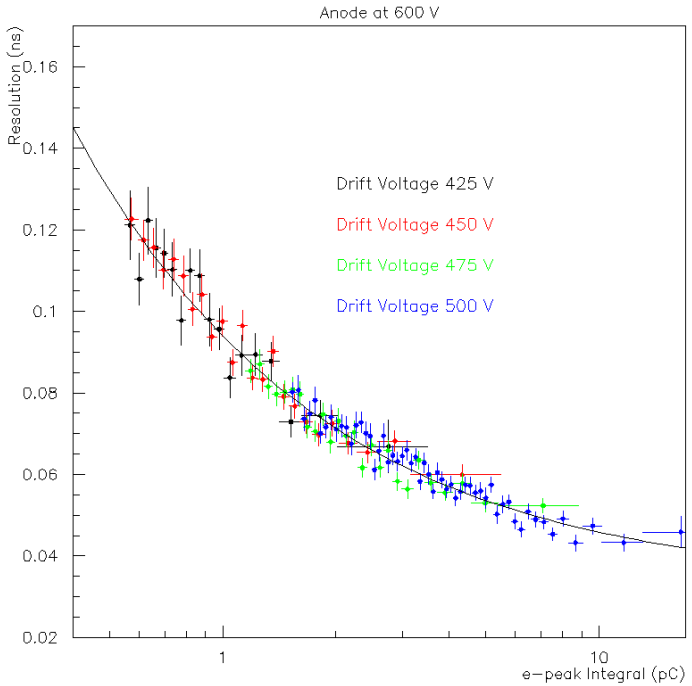

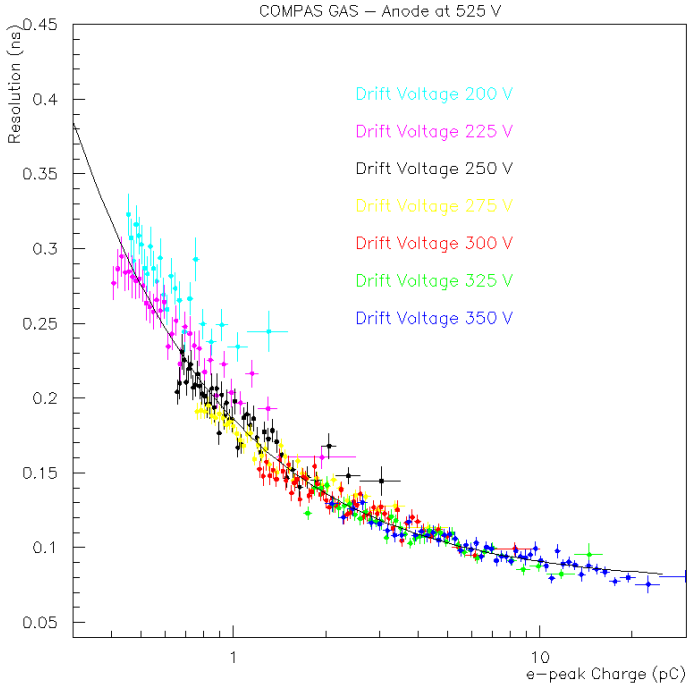

$$f(x) = \frac{b}{x^w} + a$$

CF_4+20%C_2H_6 at 0.5 bar

"Compass gas" (Ne+10%C_2H_6+10%CF_4) at 1 bar.

Figure 10: *The slewing corrections (i.e. the mean ΔT after subtracting the constant term) and the timing resolution vs the e-peak charge (top plots) and the e-peak amplitude (bottom plots) for all the calibration data collected with CF4 gas filling. The red points correspond to data collected with 600 V at the anode and different (425 V, 450 V, 475 V, 500 V) drift voltage settings, the green points correspond to data with 625 V at the anode and drift voltage set to 350 V, 375 V, 400 V, 425 V, whilst the blue points represent measurements using data collected with 650 V anode voltage and drift voltages set to 350 V, 375 V, 400 V , 425 V and 450V.*

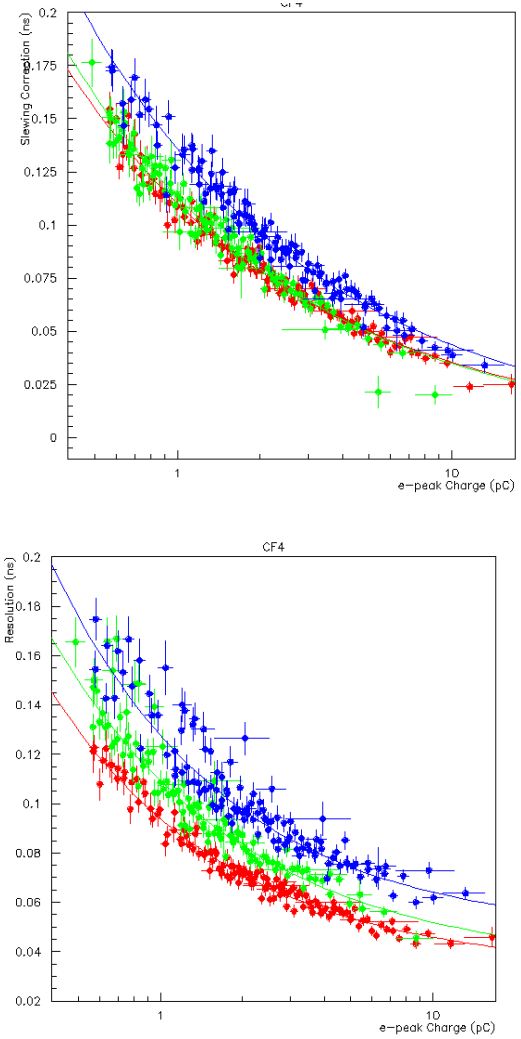

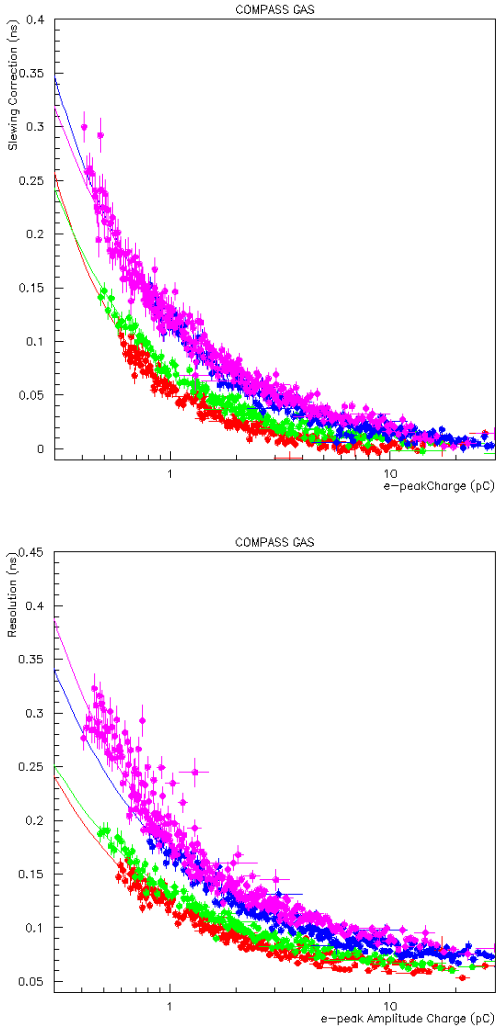

Figure 11 *: The slewing corrections (i.e. the mean ΔT after subtracting the constant term) and the timing resolution vs the e-peak charge (top plots) and the e-peak amplitude (bottom plots) for all the calibration data collected with COMPASS gas filling. The red points correspond to data collected with 450 V at the anode and different (300 V, 325 V, 350 V, 375 V, 400 V and 425V) drift voltage settings, the green points correspond to data with 475 V at the anode and drift voltage set to 300 V, 325 V, 350 V, 375 V and 400V, the blue points represent measurements using data collected with 500 V anode voltage and drift voltages set to 275 V, 300 V, 325 V, 350 V, 375V, 400 V and 450V, whilst the purple points are measurements using data sets taken with 525 V at the anode and the drift voltage set at 200V, 225 V, 275 V, 300 V, 325 V and 350 V*

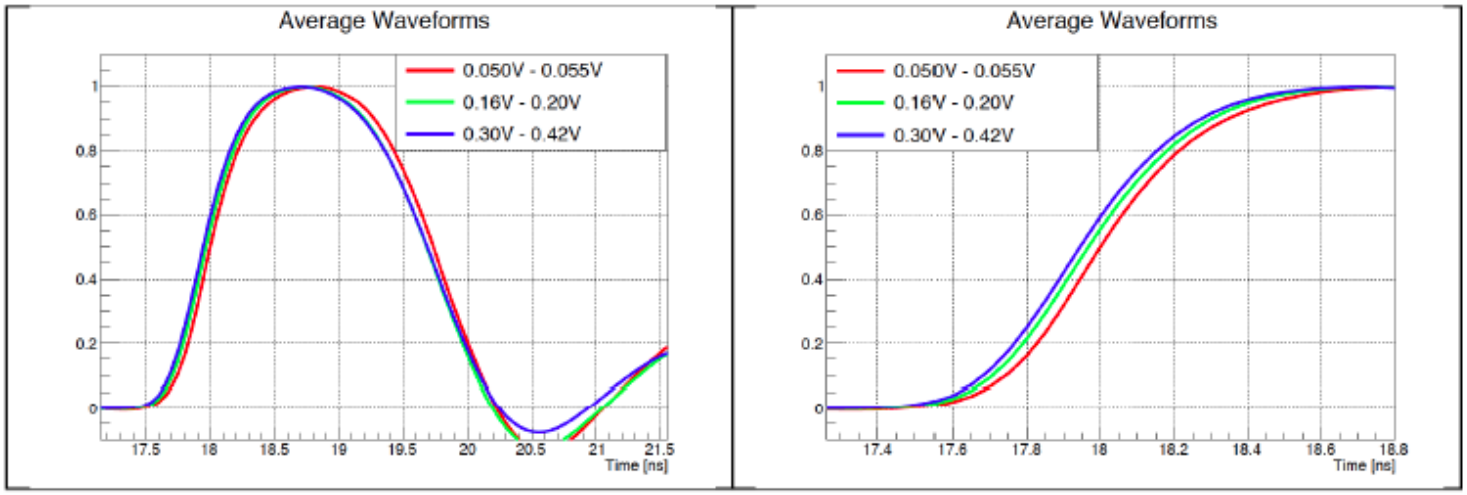

Figure 1.6: Average waveforms, normalized to unity electron peak amplitude, in three different bins of electron peak amplitude. The right plot shows the same thing as the left one, but focused on the leading edges. Red corresponds to events with electron peak amplitudes in the range $[0.050\ V, 0.055\ V]$, green to those in $[0.16\ V, 0.20\ V]$, and blue to those in $[0.30\ V, 0.42\ V]$.

This simulation is based in Garfield++ using Magboltz.The electric field is modeled using ANSYS.However, while the real mesh is woven and calendered, the mesh model in this simulation is **only woven** and not calendered.

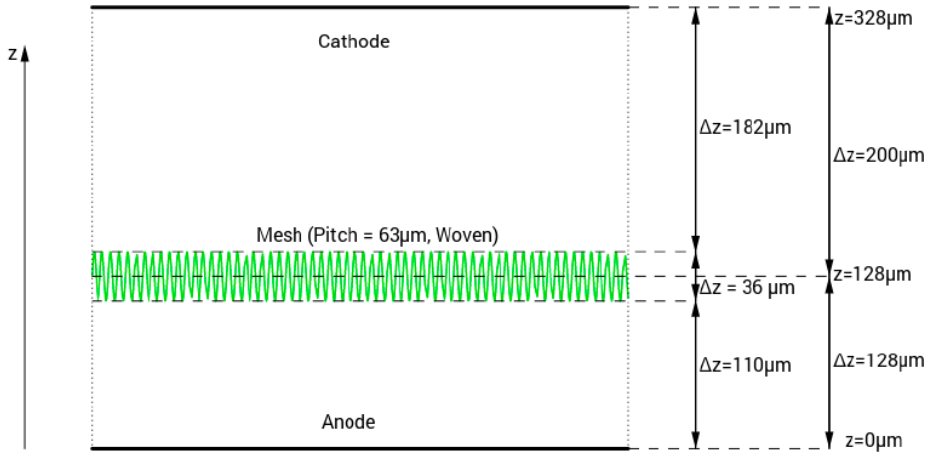

Figure 2.1: Diagram of the simulated detector model. The geometry is periodic in the plane that is perpendicular to the z-axis (electric field). The reference $z = 0$ is the anode.

Stage 1: Simulation of the pre-amplification region.

Stage 2: Simulation of the amplification region.

Stage 3: Combination of Stage 1. and Stage 2., and convolution with the parametrization of the electronics' response to generate waveforms.

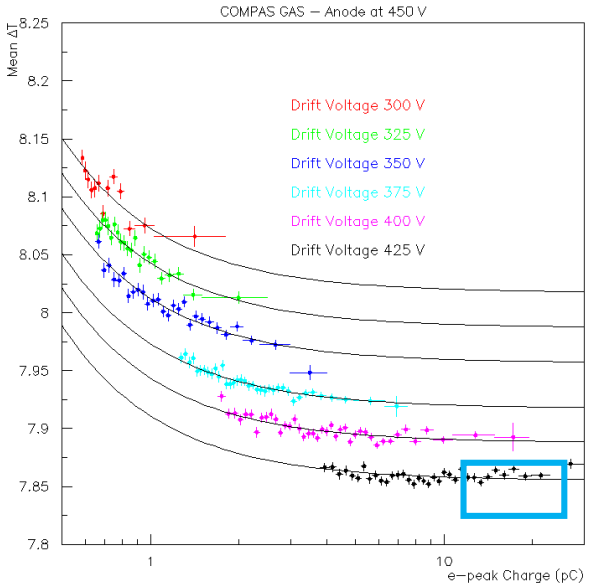

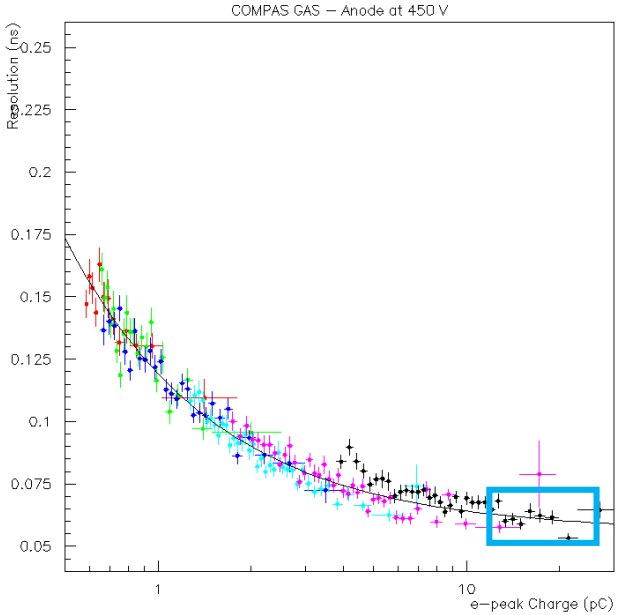

Parameterize the pulse shape corresponding to a single electron avalanche (s.e.a) in the amplification region as:

$$f(t; p_0, p_1, p_2, p_3, p_4, p_5, p_6) = \frac{p_0}{\left(1 + e^{-(t-p_1)p_2}\right)^{p_3}} - \frac{p_0}{\left(1 + e^{-(t-p_4)p_5}\right)^{p_6}}$$

Use the simulation of the preamplification region and the s.e.a. pulse shape to fit the mean e-peak waveform obtained by averaging experimental events

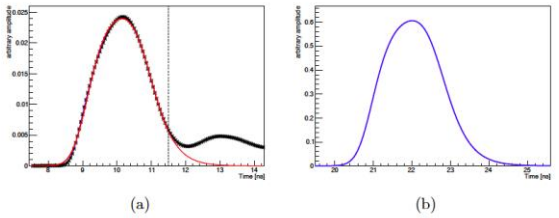

(a) (b)

Figure 2.7: (a) The black points in the right plot correspond to the experimental average waveform for events with an electron peak charge above 15. pC. This region was chosen to prevent the SAT dependence from affecting the result. The fit result is shown in the red line of the plot. The dashed line corresponds to the right limit of the fit region. (b) The final impulse response as a function of time is shown.

The shapes of the simulated pulses, for different drift voltages (same anode voltages) and for different e-peak sizes, agree very well with the data

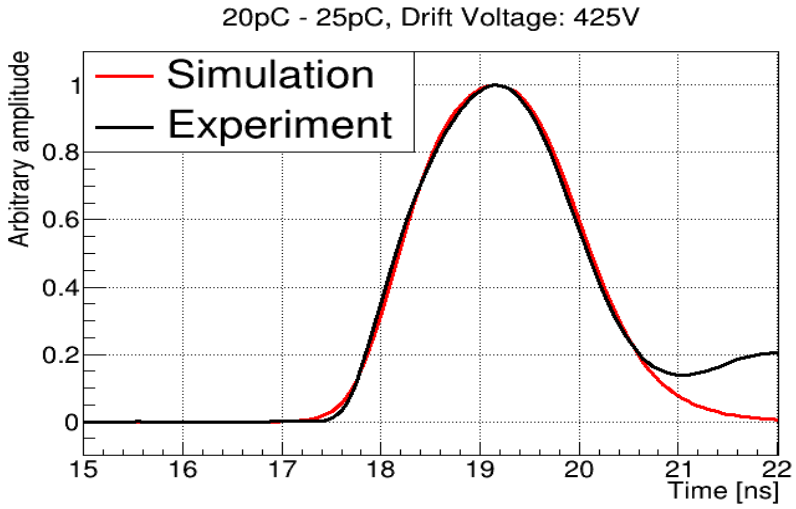

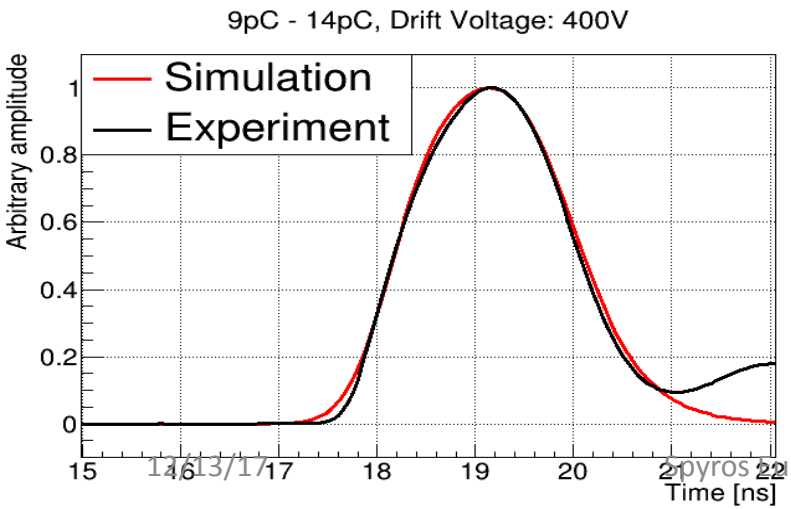

The worst case – perhaps due to noise/reflections contributions

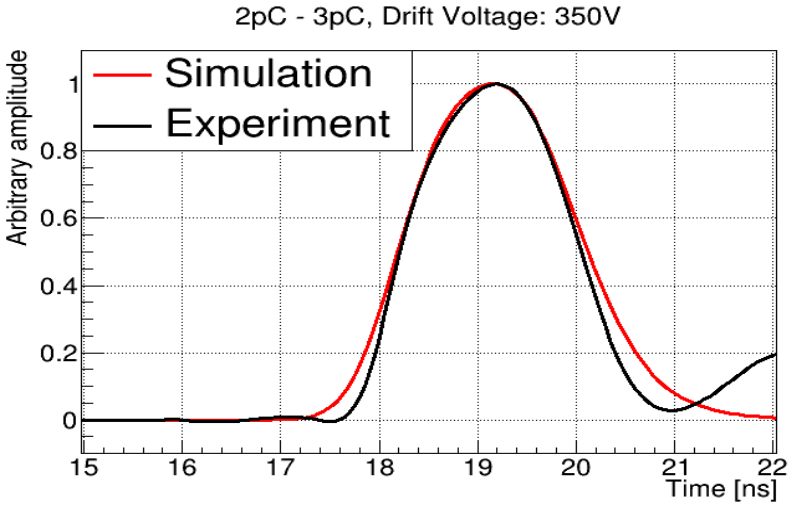

We have to scale the MC charge (or amplitude) predicted distributions in order to take into account the electronics' gains. We expected that by adjusting the scale factor at some drift operating voltage we should predict all the other distributions of events collected with the same anode but different drift voltages, WITHOUT any extra fine tuning.

However…

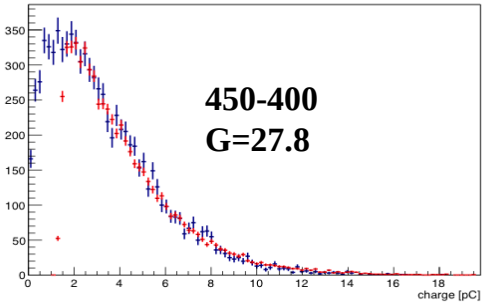

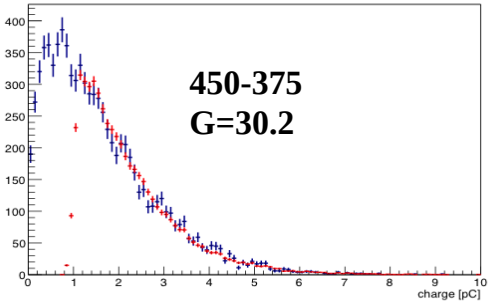

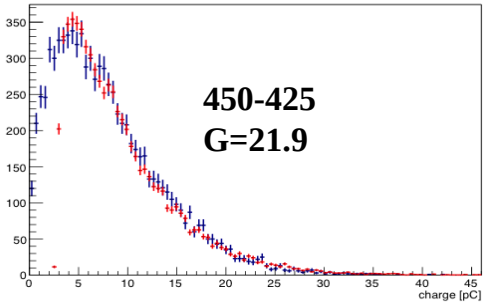

It is known that the COMPASS gas mixture has a significant penning effect. Until now this effect was ignored in the simulation. We consider different penning transfer rates to examine its behaviour.

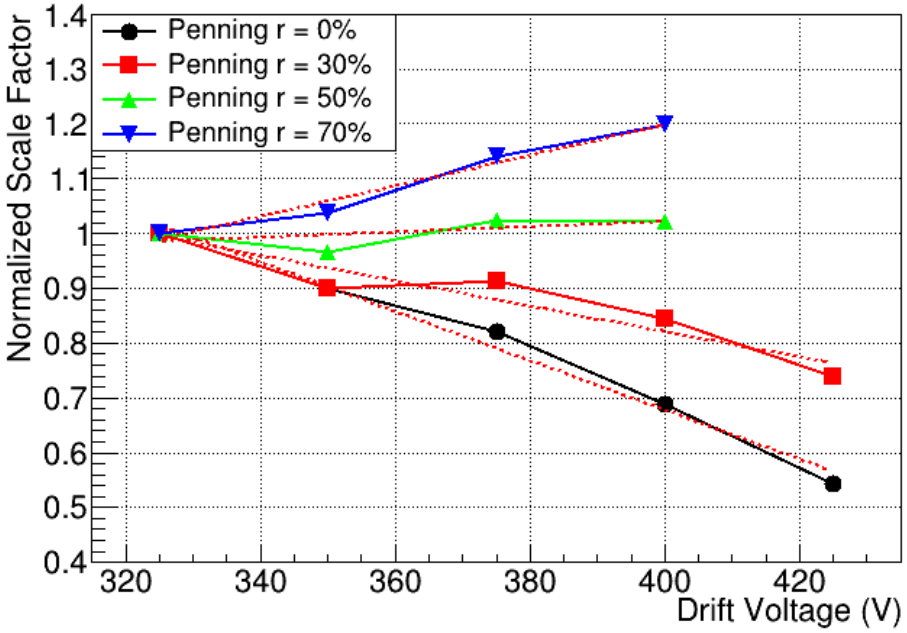

Approximately, for a transfer rate r ≈ 50%, the scale factor is not dependent on the drift voltage setting.

Fig: Scale factor, G, as a function of drift voltage, divided by the scale factor at 325 V. Red lines dashed represent linear fits.

Signal Arrival Time

Simulation

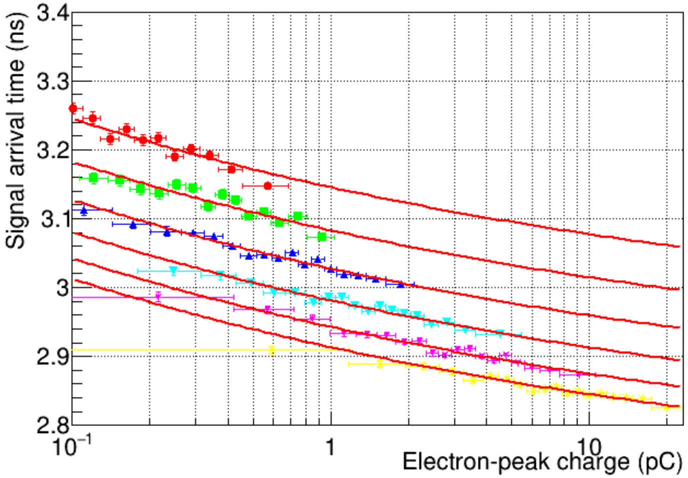

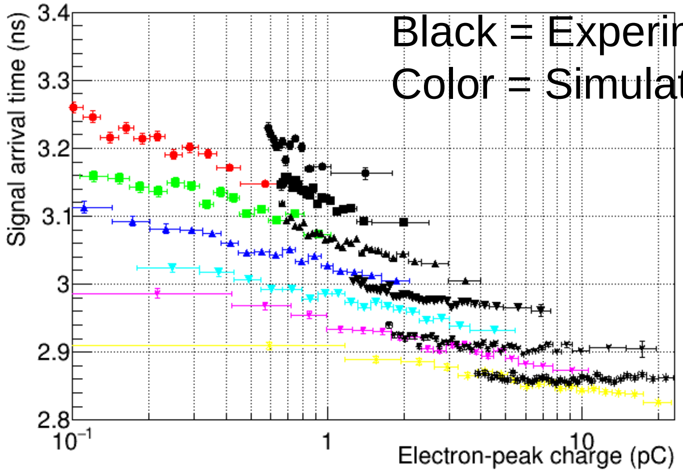

Experiment

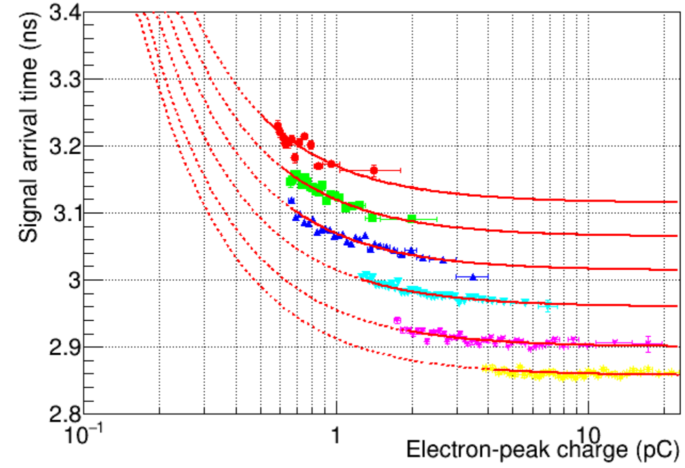

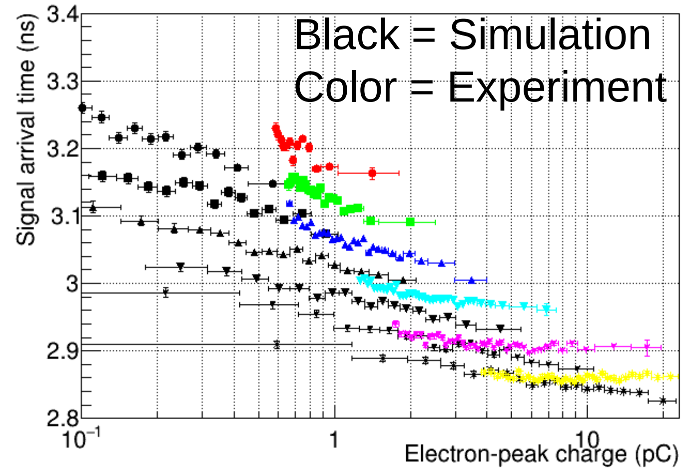

The simulation predicts the dependence of the signal arrival time on the e-peak size, as observed in the data. However, the simulation prediction does not coincide with the observed dependence.

There is not any electronic noise in the simulation

Timing Resolution

Simulation

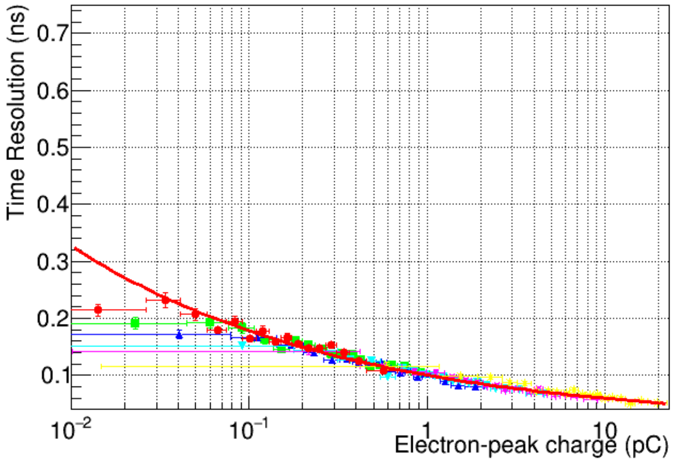

Experiment

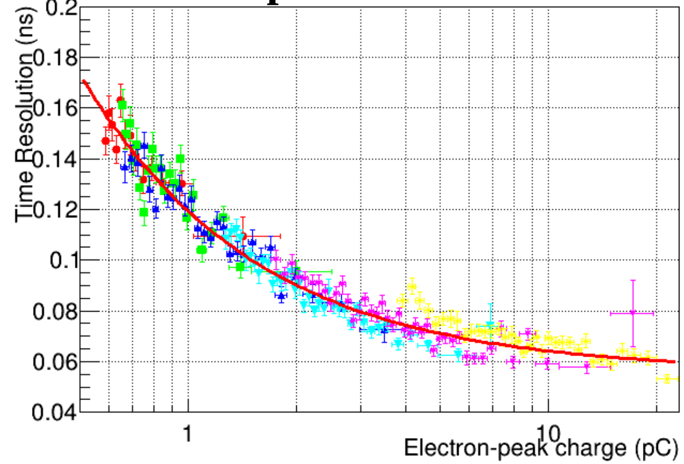

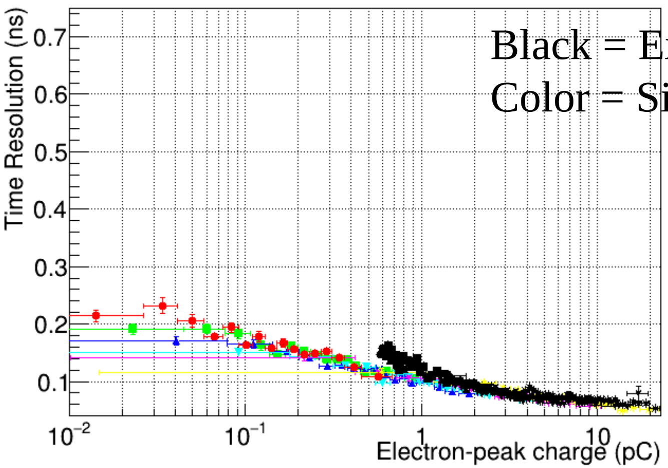

Black = Experiment
Color = Simulation

Black = Simulation
Color = Experiment

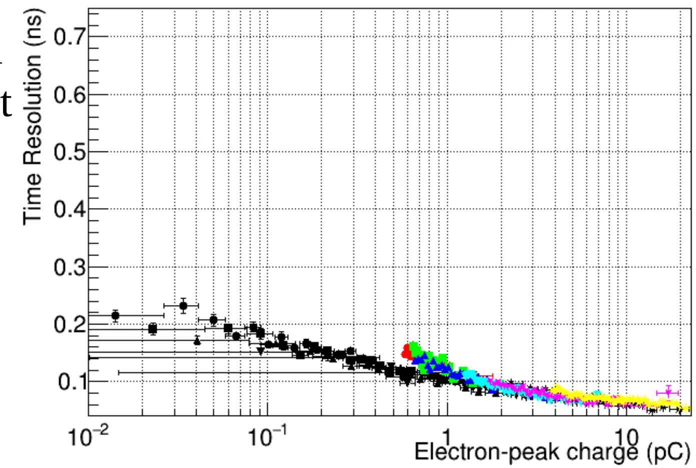

The simulation predicts a dependence of the timing resolution on the e-peak size, as observed in the data. However, the simulation prediction does not coincide with the observed dependence.

There is not any electronic noise in the simulation

Furthermore, the simulation predicts that large pulses are arriving earlier than smaller pulses whilst the pulse shape remains almost the same, as it has been observed in the data.

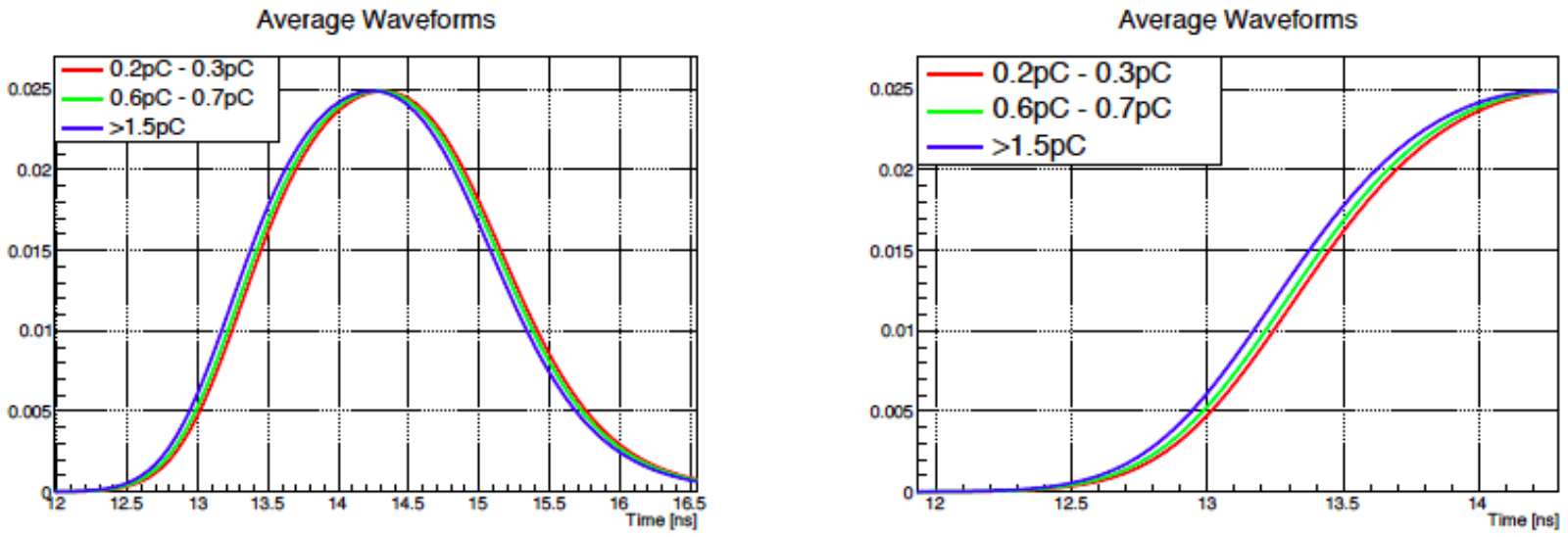

Figure 2.12: Both figures show the average simulated waveforms in different bins of electron peak charge, denoted by the color code. In (a), the whole electron peak is shown, whilst in (b) the focus is on the leading edge.

Include electronic noise in the simulation

Signal Arrival Time

Simulation

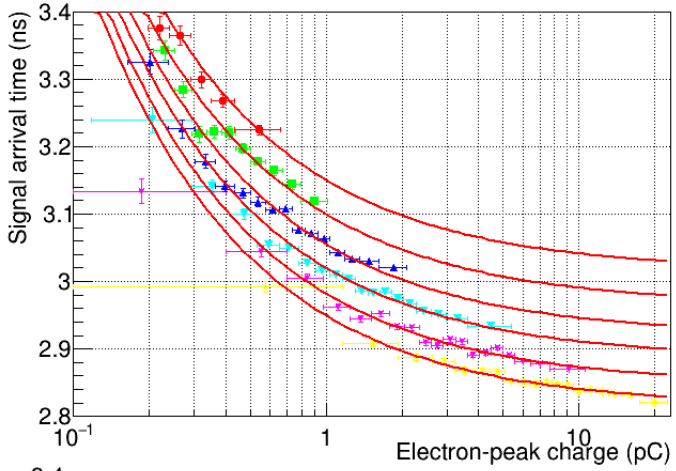

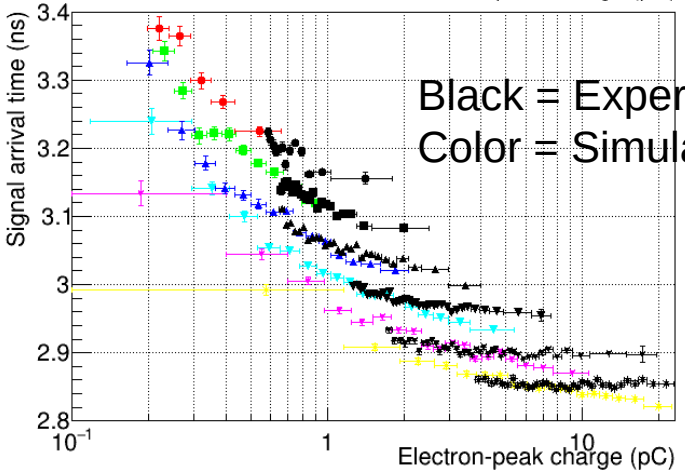

Experiment

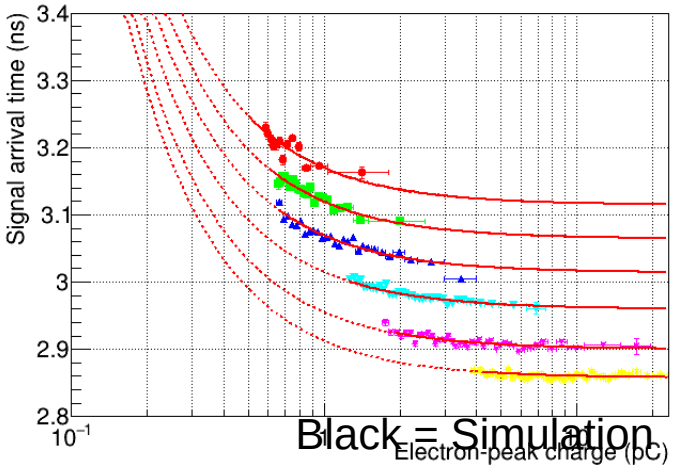

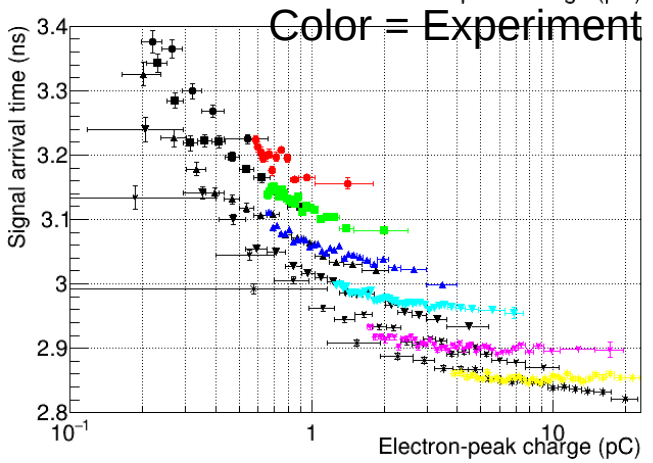

A simple 2.5mV RMS, uncorrelated noise inclusion makes the simulation's predictions to agree much better with the experiment.

Include electronic noise in the simulation

Timing Resolution

Simulation

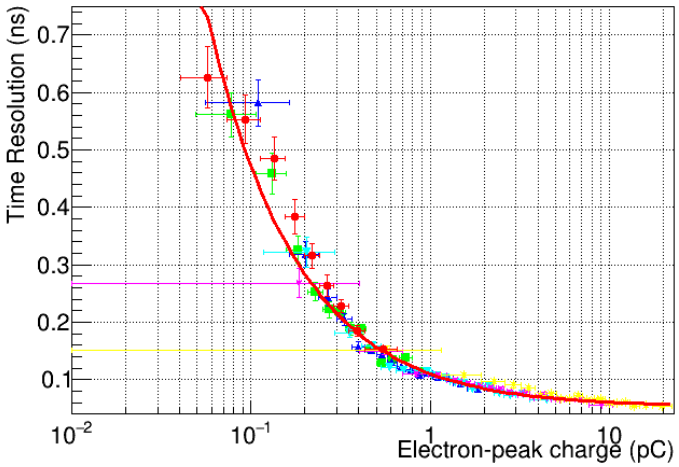

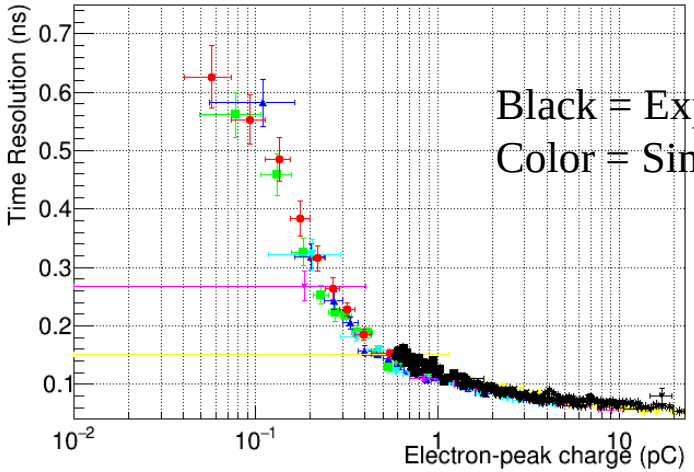

Black = Experiment
Color = Simulation

Experiment

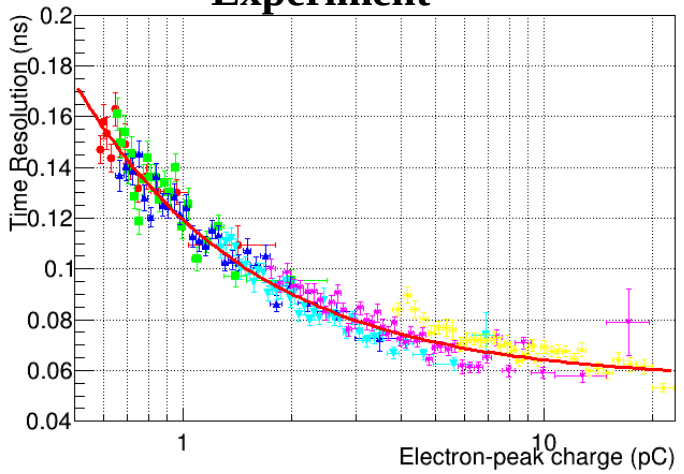

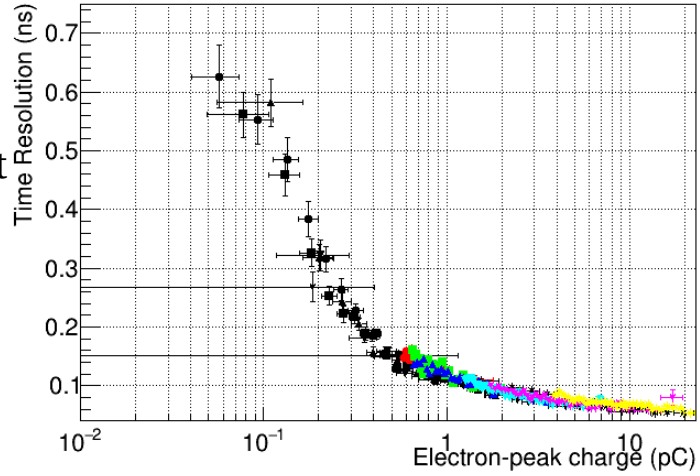

Black = Simulation
Color = Experiment

The simple 2.5mV RMS noise inclusion makes the simulation's resolution agree almost perfectly with the experiment.

Inverse Engineering

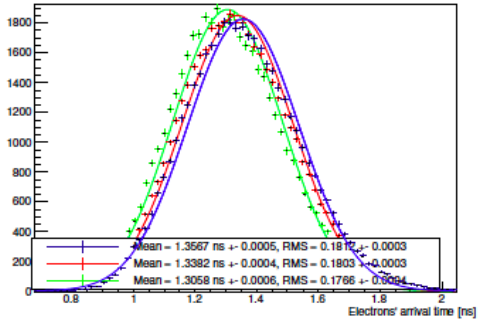

Figure 3.2: Distribution of the arrival times of electrons when their number is in the range of (blue) $[5, 10]$, (red) $[10, 15]$, (green) $[30, 35]$. The heights of the distributions have been scaled for visual purposes.

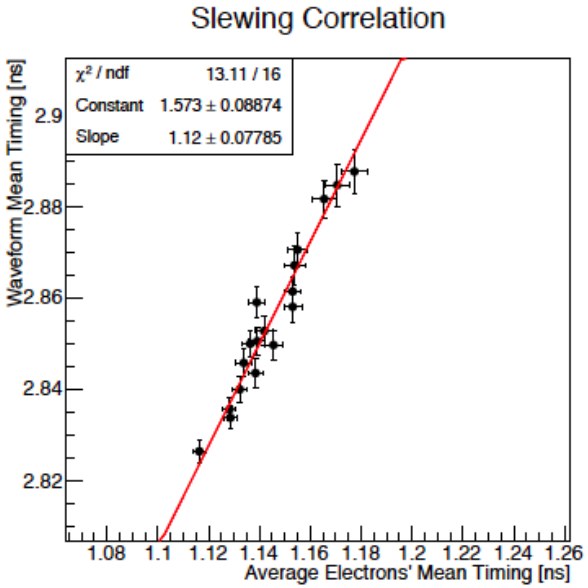

(a)

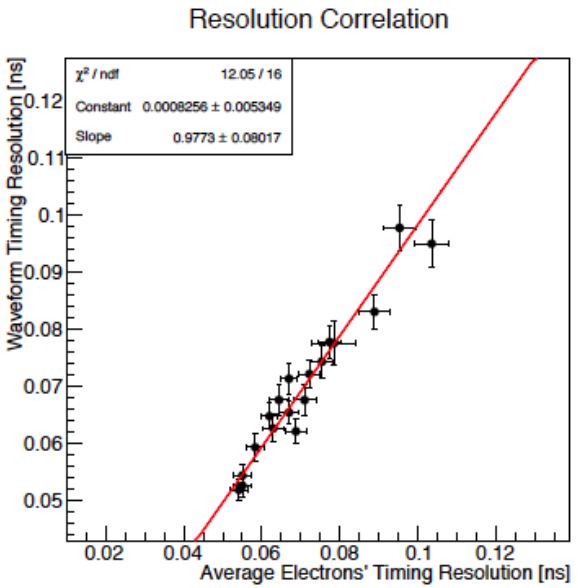

(b)

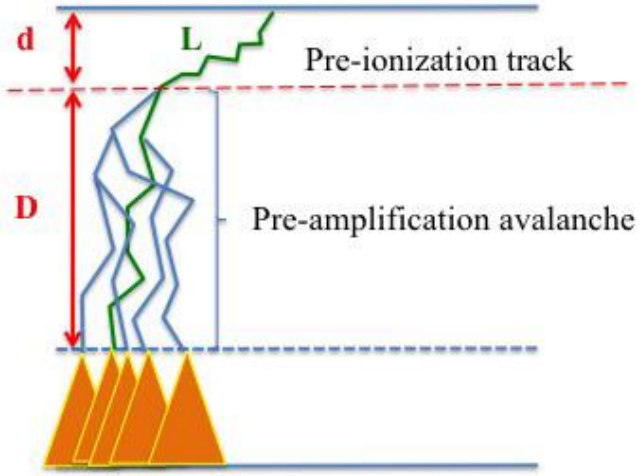

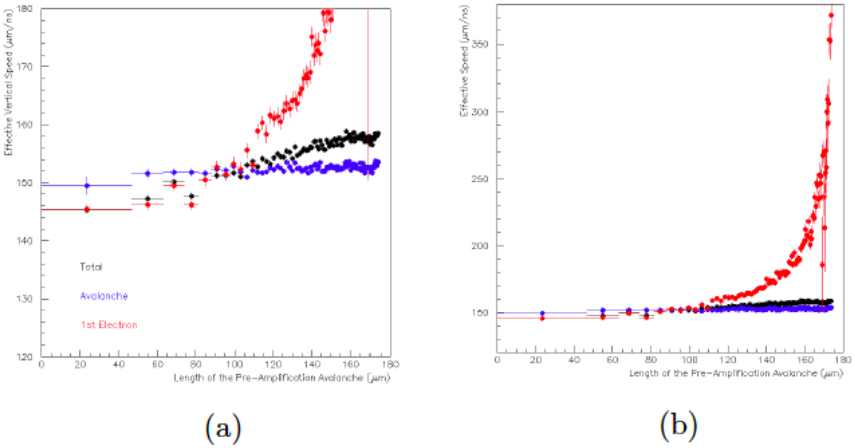

(a) (b)

see K. Paraschou talk

Figure 3.11: Both figures show the mean effective total velocity as a function of the pre-amplification avalanche length. Both show the same data points but (a) shows the full range while (b) is focused on a smaller range in the mean effective total speed for a clearer view. Black corresponds to the total speed, blue to the avalanche's and red to the initial photoelectron's.